

ELECTRONIC SUPPLEMENTARY INFORMATION (ESI)

Metal coordination induced ring contraction of porphyrin derivatives

Bratati Patra,^a Sebastian Sobottka,^b Sruti Mondal,^a Biprajit Sarkar,^{*b} and Sanjib Kar^{*a}

^aSchool of Chemical Sciences, National Institute of Science Education and Research (NISER), Bhubaneswar, Khordha, 752050, India and Homi Bhabha National Institute, Training School Complex, Anushakti Nagar, Mumbai, 400 094, India,

E-mail: sanjib@niser.ac.in

^bInstitut für Chemie und Biochemie, Anorganische Chemie, Freie Universität Berlin, Fabeckstraße 34-36, D-14195, Berlin, Germany.

E-mail: biprajit.sarkar@fu-berlin.de

Experimental Section

Materials

The precursors pyrrole, *p*-chloranil, 4-Cyano benzaldehyde, 4-Nitro benzaldehyde, Ferrocenecarboxaldehyde and TBAP (Tetrabutyl ammonium perchlorate) were purchased from Aldrich, USA. Cu(OAc)₂ and Ag(OAc) were purchased from Merck, India. Other chemicals were of reagent grade. Hexane and CH₂Cl₂ were distilled from KOH and CaH₂ respectively. For spectroscopy and electrochemical studies HPLC grade solvents were used.

Physical Measurements

UV–Vis spectral studies were performed on a Perkin–Elmer LAMBDA-750 spectrophotometer. The elemental analyses were carried out with a Perkin–Elmer 240C elemental analyzer. The NMR measurements were carried out using a Bruker AVANCE 400 and 700 NMR spectrometer. Tetramethylsilane (TMS) was the internal standard. Electrospray mass spectra were recorded on a Bruker Micro TOF-QII mass spectrometer. GC–EIMS spectra were taken on a Thermo Scientific ITQ 900 spectrometer. Cyclic voltammetry measurements were carried out using a CH Instruments model CHI1120A electrochemistry system. A glassy–carbon working electrode, a platinum wire as an auxiliary electrode and a saturated calomel reference electrode (SCE) were used in a three–electrode configuration. Tetrabutyl ammonium perchlorate (TBAP) was the supporting electrolyte (0.1M) and the concentration of the solution was 10^{−3}M with respect to the complex. The half wave potential $E_{0.298}^0$ was set equal to $0.5(E_{pa} + E_{pc})$, where E_{pa} and E_{pc} are anodic and cathodic cyclic voltammetric peak potentials, respectively. The scan rate used was 100 mV s^{−1}. EPR spectra in the X band were recorded with a Bruker System EMX. Simulations of EPR spectra were done using the Simfonia program.

Crystal Structure Determination

Single crystals of **3** and **5** were grown by slow diffusion of a solution of the **3** and **5** in dichloromethane into hexane, followed by slow evaporation under atmospheric conditions. The crystal data of **3** and **5** were collected on a Bruker Kappa APEX II CCD diffractometer at 293 K and a Rigaku Oxford diffractometer at 293 K respectively. Selected data collection parameters and other crystallographic results are summarized in Table S1. All data were corrected for Lorentz polarization and absorption effects. The program package SHELXTL¹ was used for structure solution and full matrix least squares refinement on F². Hydrogen

atoms were included in the refinement using the riding model. Contributions of H atoms for the water molecules were included but were not fixed. Disordered solvent molecules were taken out using SQUEEZE command in PLATON.²

CCDC 1842435-1842436 contain the supplementary crystallographic data for **3** and **5**. These data can be obtained free of charge via www.ccdc.cam.ac.uk/data_request/cif.

Syntheses

Synthesis of 5,15-diferrocenyl-10,20-bis(4-cyanophenyl)porphyrin, **1**:

The *trans*-ferrocenyl-porphyrin (**1-2**) were prepared by slight modification of a general synthetic procedure developed earlier by Gryko *et al.* for the synthesis of F B corrole derivatives.³ Hence, only one representative case is discussed below. 5-(4-Cyanophenyl)dipyrromethane (247 mg, 1 mmol) and Ferrocene carboxaldehyde (107mg, 0.5mmole) were dissolved in 1:1 MeOH/H₂O (100 mL) mixture. The reaction was kept for stirring for 1 h in presence of dil. HCl and then was extracted with CHCl₃. The organic layer was washed twice with H₂O, dried by anhydrous Na₂SO₄, filtered, and diluted to 250 mL with CHCl₃. Then *p*-chloranil (360 mg, 1.5 mmol) was added, and the mixture was stirred for 10 min. The solvent was removed by rotary evaporation and the yellowish green colored crude product was purified by column chromatography through silica gel (100–200 mesh) with 65% CH₂Cl₂ and 35% hexane as eluent.

For 5,15-diferrocenyl-10,20-bis(4-cyanophenyl)porphyrin, **1**:

Yield: 8% (0.035 g). Anal. Calcd (found) for C₅₄H₃₆Fe₂N₆ (**1**): C, 73.65 (73.78); H, 4.12 (4.22); N, 9.54 (9.46). λ_{max} / nm (ϵ /M⁻¹cm⁻¹) in dichloromethane: 427 (195000), 593 (15000), 690 (16000). (Fig. S12, Table S2). ¹H NMR (400 MHz, Chloroform-*d*) δ 9.87 (d, *J* = 4.8 Hz, 4H, β -pyrrole), 8.55 (d, *J* = 4.9 Hz, 4H, β -pyrrole), 8.30 (d, *J* = 8.1 Hz, 4H, aryl-H), 8.07 (d, *J* = 8.2 Hz, 4H, aryl-H), 5.50 (t, *J* = 1.9 Hz, 4H, Fc-H), 4.85 (t, *J* = 1.8 Hz, 4H, Fc-H), 4.13 (s, 10H, Fc-H), -1.67 (s, 2H, Por-NH) (Fig. S1). ¹³C NMR (101 MHz, CDCl₃) δ 147.49, 138.39, 137.86, 135.04, 132.00, 131.58, 131.50, 130.65, 130.10, 128.62, 126.85, 126.07, 119.21, 117.62, 112.02, 71.62, 70.81, 69.65, 69.21, 68.50 (Fig. S2). The electrospray mass spectrum in acetonitrile showed peaks centred at *m/z* = 880.17 correspond to [**1**]⁺ (880.17 calcd for C₅₄H₃₆Fe₂N₆) {Fig. S7}.

For 5,15-diferrocenyl-10,20-bis(4-nitrophenyl)porphyrin, ⁴ 2:

All the analytical data are consistent with literature values.⁴ Yield: 8% (0.036 g). Anal. Calcd (found) for C₅₂H₃₆Fe₂N₆O₄ (**2**): C, 67.84 (67.75); H, 3.94 (3.86); N, 9.13 (9.03). λ_{\max}/nm ($\epsilon/\text{M}^{-1}\text{cm}^{-1}$) in dichloromethane: 428 (93000), 606 (18500), 695 (19000). {Table S2}. ¹H NMR (700 MHz, Chloroform-*d*) δ 9.88 (s, 4H, β -pyrrole), 8.65 (d, $J = 7.8$ Hz, 4H, aryl-H), 8.57 (d, $J = 4.6$ Hz, 4H, β -pyrrole), 8.36 (d, $J = 7.8$ Hz, 4H, aryl-H), 5.50 (s, 4H, Fc-H), 4.86 (s, 4H, Fc-H), 4.13 (s, 10H, Fc-H), -1.64 (s, 2H, Por-NH). The electrospray mass spectrum in acetonitrile showed peaks centred at $m/z = 921.15$ correspond to [**2+H**]⁺ (920.15 calcd for C₅₂H₃₆Fe₂N₆O₄).

Synthesis of 5,15-diferrocenyl-10,20-bis(4-cyanophenyl)porphyrinato-Cu(II), 3:

0.050 g of 5,15-diferrocenyl-10,20-bis(4-cyanophenyl)porphyrin, **1** (0.056 mmol) was dissolved in 10 mL of dichloromethane and subsequently 0.046 g of copper acetate hydrate (0.24 mmol) was added to it. Then triethylamine (34 mL) was added to the reaction mixture and it was stirred for 1 hour at room temperature during which the colour changed from yellowish green to dark brown. The solvent was then removed by rotary evaporation and the brown crude product was purified by column chromatography through silica gel (100-200 mesh) column with 55% CH₂Cl₂ and 45% hexane as eluent. Subsequent recrystallization (CH₂Cl₂/hexane) gave the pure crystalline **3**.

For 5,15-diferrocenyl-10,20-bis(4-cyanophenyl)porphyrinato-Cu(II), 3:

Yield: 80% (0.043 g). Anal. Calcd (found) for C₅₄H₃₄CuFe₂N₆ (**3**): C, 68.84 (68.95); H, 3.64 (3.51); N, 8.92 (8.99). λ_{\max}/nm ($\epsilon/\text{M}^{-1}\text{cm}^{-1}$) in dichloromethane: 423 (115000), 642 (7500) { Fig. S13, Table S2}. The electrospray mass spectrum in acetonitrile showed peaks centred at $m/z = 941.06$ correspond to [**3**]⁺ (941.08 calcd for C₅₄H₃₄CuFe₂N₆) { Fig. S8}.

For 5,15-diferrocenyl-10,20-bis(4-nitrophenyl)porphyrinato-Cu(II), 4:

Yield: 79% (0.042g). Anal. Calcd (found) for C₅₂H₃₄CuFe₂N₆O₄ (**4**): C, 63.59 (63.71); H, 3.49 (3.60); N, 8.56 (8.44). λ_{\max}/nm ($\epsilon/\text{M}^{-1}\text{cm}^{-1}$) in dichloromethane: 423 (108000), 653 (13000) { Fig. S14, Table S2}. The electrospray mass spectrum in acetonitrile showed peaks centred at $m/z = 981.07$ correspond to [**4**]⁺ (981.06 calcd for C₅₂H₃₄CuFe₂N₆O₄) { Fig. S9}.

Synthesis of 10-ferrocenyl-5,15-bis(4-cyanophenyl)corrolato-Ag(III), **5**:

0.050 g of 5,15-diferrocenyl-10,20-bis(4-cyanophenyl)porphyrin, **1** (0.057 mmol) was dissolved in 10 mL of dichloromethane and subsequently 0.096 g of silver acetate (0.57 mmol) was added to it. Then triethylamine (34 mL) was added to the reaction mixture and it was stirred for 30 minutes at room temperature during which the colour changed from yellowish green to deep green. The solvent was then removed by rotary evaporation and the deep green crude product was purified by column chromatography immediately through alumina oxide active neutral column with 50% CH₂Cl₂ and 50% hexane as eluent. Subsequent recrystallization (CH₂Cl₂/hexane) gave the pure crystalline **5**.

For 10-ferrocenyl-5,15-bis(4-cyanophenyl)corrolato-Ag(III), **5**:

Yield: 85% (0.038 g). Anal. Calcd (found) for C₄₃H₂₅AgFeN₆ (**5**): C, 65.42 (65.33); H, 3.19 (3.34); N, 10.65 (10.51). λ_{\max}/nm ($\epsilon/\text{M}^{-1}\text{cm}^{-1}$) in dichloromethane: 431 (98000), 541 (11000), 571 (11000), 612 (16000) { Fig. S15, Table S2}. ¹H NMR (400 MHz, Chloroform-*d*) δ 9.87 (s, 2H, β -pyrrole), 9.07 (d, $J = 4.2$ Hz, 2H, β -pyrrole), 8.82 (d, $J = 4.5$ Hz, 2H, β -pyrrole), 8.55 (d, $J = 4.0$ Hz, 2H, β -pyrrole), 8.38 (d, $J = 7.8$ Hz, 4H, aryl-H), 8.13 (d, $J = 7.7$ Hz, 4H, aryl-H), 5.59 (s, 2H, Fc-H), 4.88 (s, 2H, Fc-H), 4.30 (s, 5H, Fc-H) { Fig. S3}. ¹³C NMR (101 MHz, CDCl₃) δ 145.30, 138.82, 136.19, 135.25, 133.97, 131.64, 130.41, 127.76, 127.63, 119.60, 119.33, 119.00, 116.57, 111.66, 75.83, 71.63, 70.68, 69.13 {Fig. S4}. The electrospray mass spectrum in acetonitrile showed peaks centred at $m/z = 788.04$ correspond to [**5**]⁺ (788.05 calcd for C₄₃H₂₅AgFeN₆) {Fig. S10}.

For 10-ferrocenyl-5,15-bis(4-nitrophenyl)corrolato-Ag(III), **6** :

Yield: 84% (0.038 g). Anal. Calcd (found) for C₄₁H₂₅AgFeN₆O₄ (**6**): C, 59.37 (59.26); H, 3.04 (3.15); N, 10.13 (10.01). λ_{\max}/nm ($\epsilon/\text{M}^{-1}\text{cm}^{-1}$) in dichloromethane: 434 (65000), 542 (9200), 577 (8800), 624 (12700) { Fig. S16, Table S2}. ¹H NMR (700 MHz, Chloroform-*d*) δ 9.89 (s, 2H, β -pyrrole), 9.11 (s, 2H, β -pyrrole), 8.85 (d, $J = 4.4$ Hz, 2H, β -pyrrole), 8.70 (d, $J = 7.8$ Hz, 4H, aryl-H), 8.59 (d, $J = 4.0$ Hz, 2H, β -pyrrole), 8.45 (d, $J = 7.9$ Hz, 4H, aryl-H), 5.62 (s, 2H, Fc-H), 4.90 (s, 2H, Fc-H), 4.31 (s, 5H, Fc-H) {Fig. S5}. ¹³C NMR (101 MHz, CDCl₃) δ 147.59, 147.23, 138.75, 136.22, 135.34, 133.90, 130.33, 127.73, 123.06, 119.68, 119.15, 116.10, 114.20, 114.10, 75.89, 71.90, 70.76, 69.24 {Fig. S6}. The electrospray mass spectrum in acetonitrile showed peaks centred at $m/z = 828.03$ correspond to [**6**]⁺ (828.03 calcd for C₄₁H₂₅AgFeN₆O₄) {Fig. S11}.

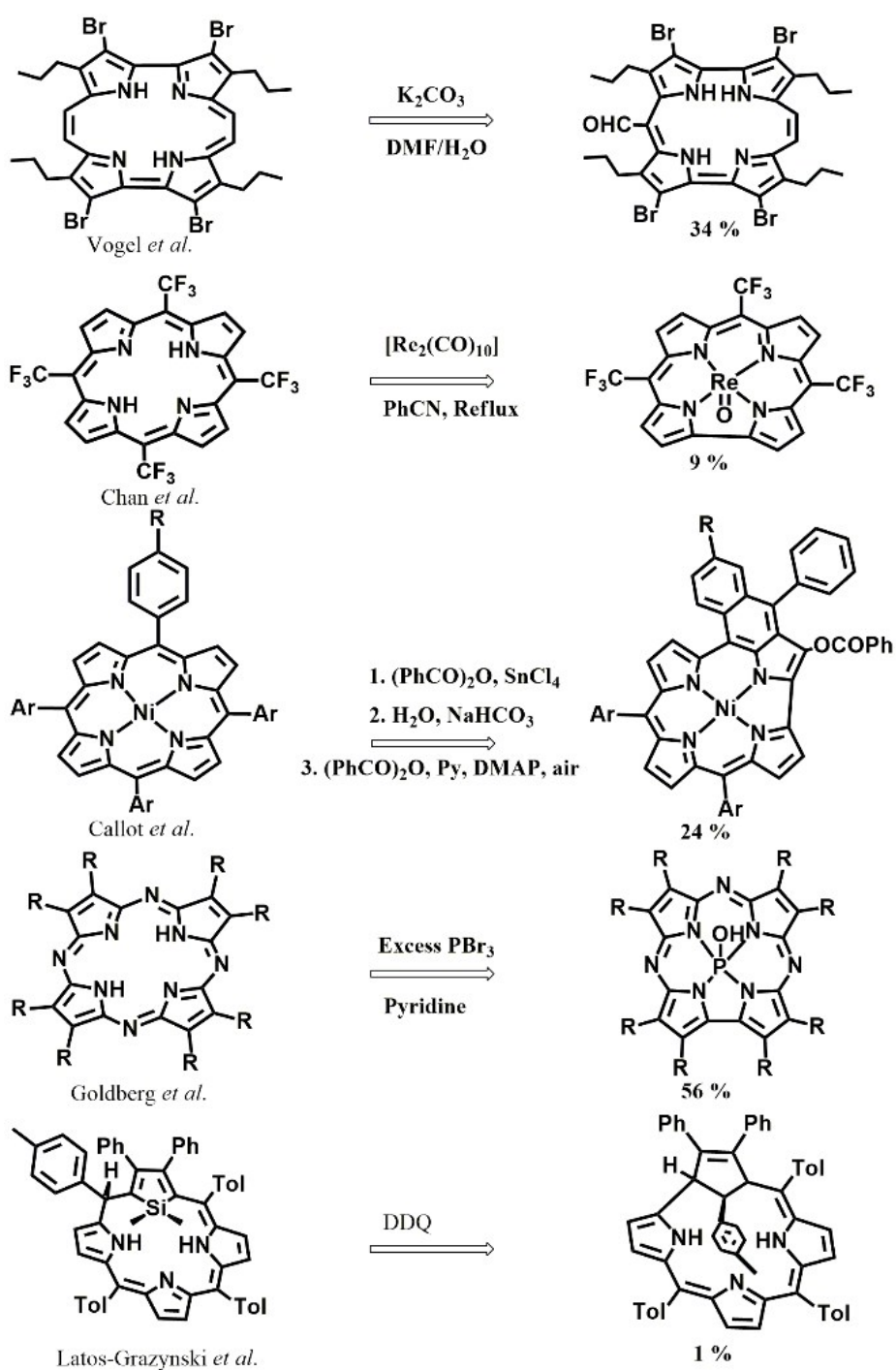
Notes and references

1. G. M. Sheldrick, *Acta Crystallogr., Sect. A: Found. Crystallogr.*, 2008, **64**, 112-122.
2. P. Van der Sluis and A. Spek, *Acta Crystallogr., Sect. A: Found. Crystallogr.*, 1990, **46**, 194-201.
3. B. Koszarna and D. T. Gryko, *J. Org. Chem.* 2006, **71**, 3707-3717.
4. P. Zhu, P. Ma, Y. Wang, Q. Wang, X. Zhao, X. Zhang, *Eur. J. Inorg. Chem.* 2011, 4241-4247.

- Scheme S1** Literature review of the previously reported cases of ring contraction.
- Fig. S1** ^1H NMR spectrum of 5,15-diferrocenyl-10,20-bis(4-cyanophenyl)porphyrin, **1** in CDCl_3 .
- Fig. S2** ^{13}C NMR spectrum of 5,15-diferrocenyl-10,20-bis(4-cyanophenyl)porphyrin, **1** in CDCl_3 .
- Fig. S3** ^1H NMR spectrum of 10-ferrocenyl-5,15-bis(4-cyanophenyl)corrolato-Ag(III), **5** in CDCl_3 .
- Fig. S4** ^{13}C NMR spectrum of 10-ferrocenyl-5,15-bis(4-cyanophenyl)corrolato-Ag(III), **5** in CDCl_3 .
- Fig. S5** ^1H NMR spectrum of 10-ferrocenyl-5,15-bis(4-nitrophenyl)corrolato-Ag(III), **6** in CDCl_3 .
- Fig. S6** ^{13}C NMR spectrum of 10-ferrocenyl-5,15-bis(4-nitrophenyl)corrolato-Ag(III), **6** in CDCl_3 .
- Fig. S7** ESI-MS spectrum of 5,15-diferrocenyl-10,20-bis(4-cyanophenyl)porphyrin, **1** in CH_3CN shows (a) the measured spectrum and (b) with isotopic distribution pattern.
- Fig. S8** ESI-MS spectrum of 5,15-diferrocenyl-10,20-bis(4-cyanophenyl)porphyrinato-Cu(II), **3** in CH_3CN shows (a) the measured spectrum and (b) with isotopic distribution pattern.
- Fig. S9** ESI-MS spectrum of 5,15-diferrocenyl-10,20-bis(4-nitrophenyl)porphyrinato-Cu(II), **4** in CH_3CN shows (a) the measured spectrum and (b) with isotopic distribution pattern.
- Fig. S10** ESI-MS spectrum of 10-ferrocenyl-5,15-bis(4-cyanophenyl)corrolato-Ag(III), **5** in CH_3CN shows (a) the measured spectrum and (b) with isotopic distribution pattern.
- Fig. S11** ESI-MS spectrum of 10-ferrocenyl-5,15-bis(4-nitrophenyl)corrolato-Ag(III), **6** in CH_3CN shows (a) the measured spectrum and (b) with isotopic distribution pattern.
- Fig. S12** Electronic absorption spectrum of **1** in dichloromethane.
- Fig. S13** Electronic absorption spectrum of **3** in dichloromethane.
- Fig. S14** Electronic absorption spectrum of **4** in dichloromethane.
- Fig. S15** Electronic absorption spectrum of **5** in dichloromethane.
- Fig. S16** Electronic absorption spectrum of **6** in dichloromethane.

- Fig. S17** Cyclic voltammograms (—) and differential pulse voltammograms (---) of **3** in CH₂Cl₂. The potentials are vs. ferrocene/ferricinium.
- Fig. S18** Cyclic voltammograms (—) and differential pulse voltammograms (---) of **5** in CH₂Cl₂. The potentials are vs. ferrocene/ferricinium.
- Fig. S19** Experimental and simulated EPR spectrum of **3** measured in DCM at room temperature.
- Fig. S20** Experimental and simulated EPR spectrum of **4** measured in DCM at room temperature.
- Fig. S21** ¹H NMR spectra of (a) pure **1** in CDCl₃, (b) the sample prepared via treatment of **1** (equimolar amount) with Ag(CH₃COO) and trimethylamine in DCM, stirred at RT for 30 mins, followed by filtration of the silver residues and the evaporation of the residual solvent containing triethylamine and dissolution in CDCl₃, and (c) pure **5** in CDCl₃.
- Fig. S22** 5,15-diferrocenyl-10,20-bis(4-cyanophenyl)porphyrin, **1** was dissolved in dichloromethane. Then triethylamine was added to the reaction mixture and it was stirred continuously at room temperature. Aliquots of this reaction mixture were taken after 15 minutes and were monitored by GC-EIMS analysis.
- Fig. S23** 5,15-diferrocenyl-10,20-bis(4-cyanophenyl)porphyrin, **1** was dissolved in dichloromethane and subsequently silver acetate was added to it. Then triethylamine was added to the reaction mixture and it was stirred continuously at room temperature. Aliquots of this reaction mixture were taken after 2 minutes and were monitored by GC-EIMS analysis.
- Fig. S24** Mass spectrum (GC-EIMS) of ferrocenyl derivatives detected by GC of the reaction mixture.
- Fig. S25** Mass spectrum (GC-EIMS) of ferrocenyl derivatives detected by GC of the reaction mixture.
- Fig. S26** 5,15-diferrocenyl-10,20-bis(4-cyanophenyl)porphyrin, **1** was dissolved in dichloromethane and subsequently silver acetate was added to it. Then triethylamine was added to the reaction mixture and it was stirred continuously at room temperature. Aliquots of this reaction mixture were taken after 30 minutes and were monitored by GC-EIMS analysis.
- Fig. S27** Mass spectrum (GC-EIMS) of ferrocenyl derivatives detected by GC of the reaction mixture.

- Fig. S28** Mass spectrum (GC-EIMS) of ferrocenyl derivatives detected by GC of the reaction mixture.
- Fig. S29** Ferrocene was dissolved in dichloromethane and were monitored by GC-EIMS analysis.
- Fig. S30** Mass spectrum (GC-EIMS) of ferrocene detected by GC of the reaction mixture.
- Fig. S31** Ferrocenecarboxaldehyde was dissolved in dichloromethane and were monitored by GC-EIMS analysis.
- Fig. S32** Mass spectrum (GC-EIMS) of ferrocenecarboxaldehyde detected by GC of the reaction mixture.
- Table S1** Crystallographic Data for **3** and **5**.
- Table S2** UV–Vis. and electrochemical data
- Table S3** Overview of g values and hyperfine coupling constants, obtained from simulation.



Scheme S1 Literature review of the previously reported cases of ring contraction.

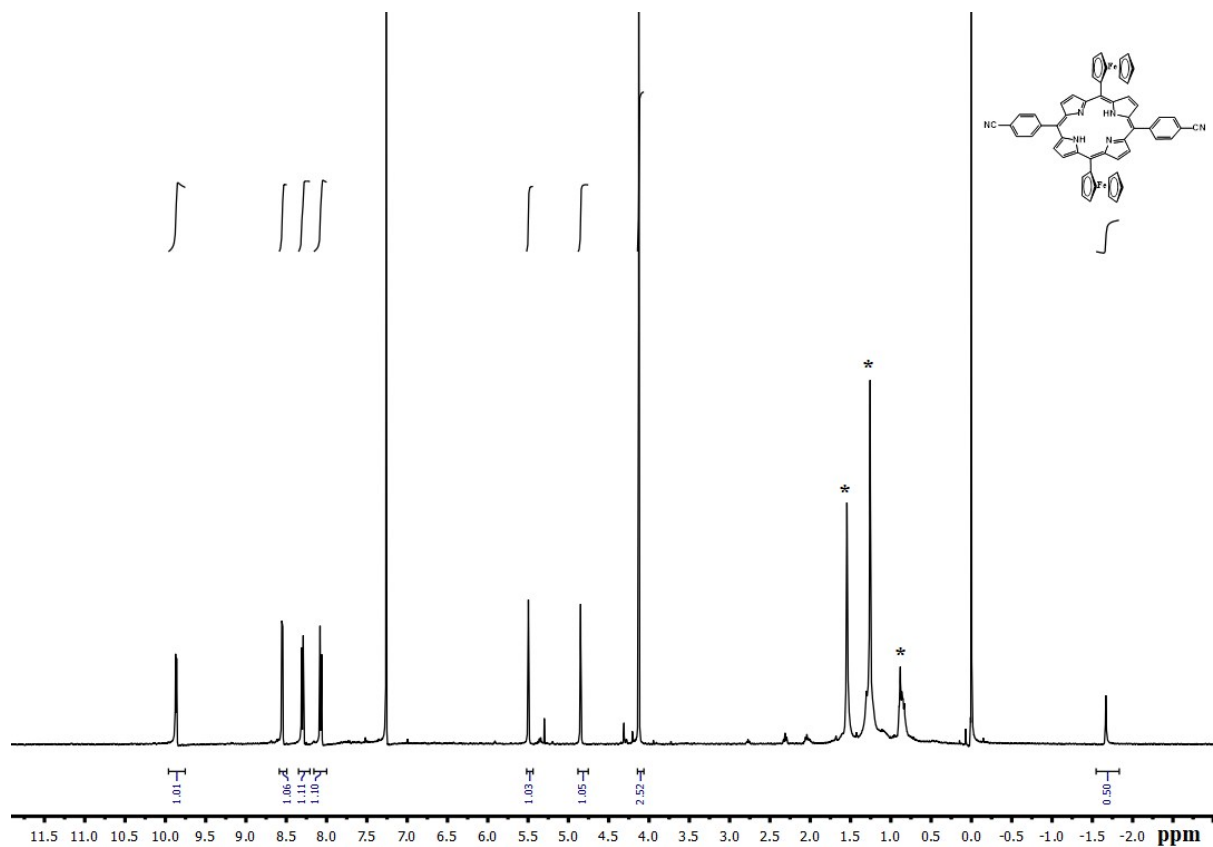


Fig. S1 ^1H NMR spectrum of 5,15-diferrocenyl-10,20-bis(4-cyanophenyl)porphyrin, **1** in CDCl_3 .

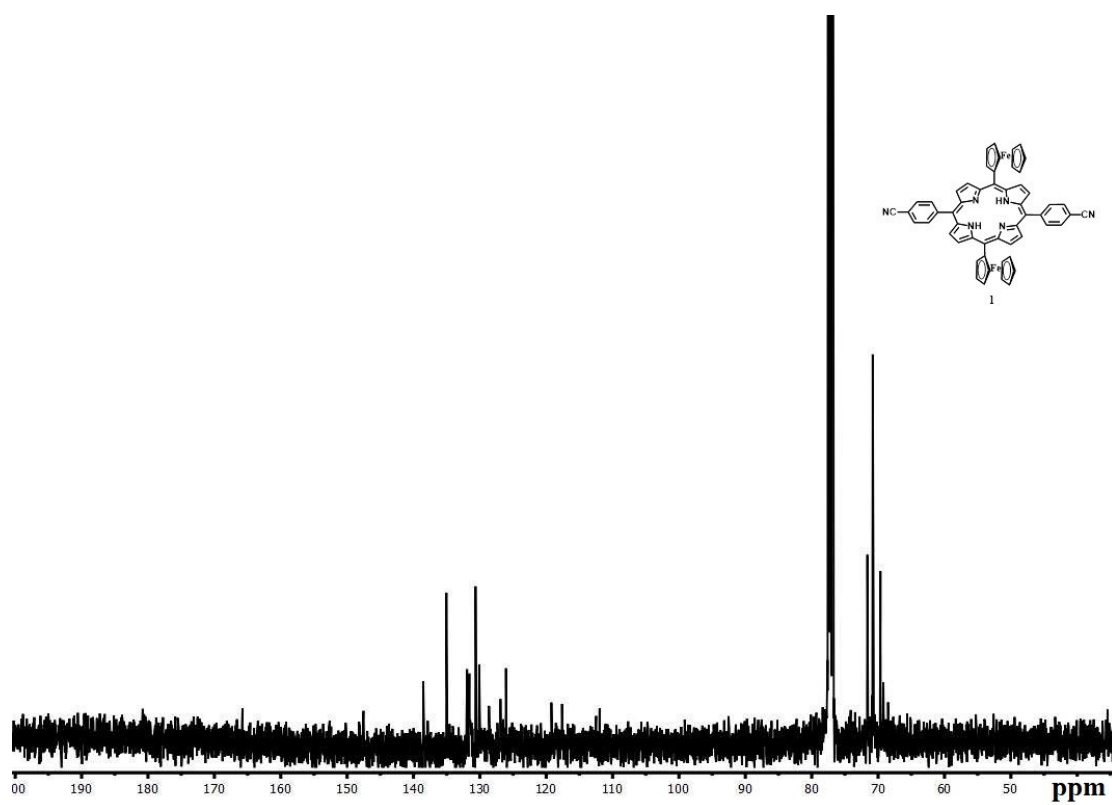


Fig. S2 ^{13}C NMR spectrum of 5,15-diferrocenyl-10,20-bis(4-cyanophenyl)porphyrin, **1** in CDCl_3 .

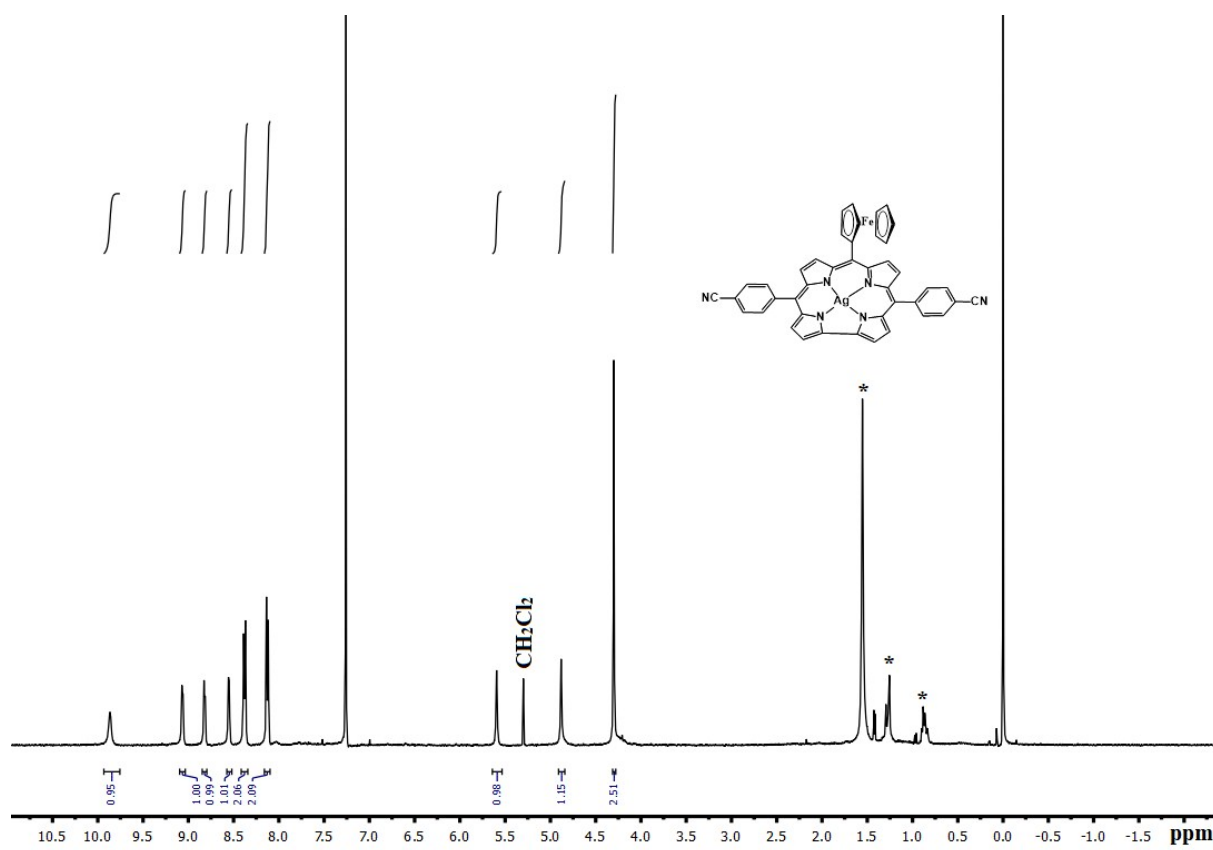


Fig. S3 ^1H NMR spectrum of 10-ferrocenyl-5,15-bis(4-cyanophenyl)corrolato-Ag(III), **5** in CDCl_3 .

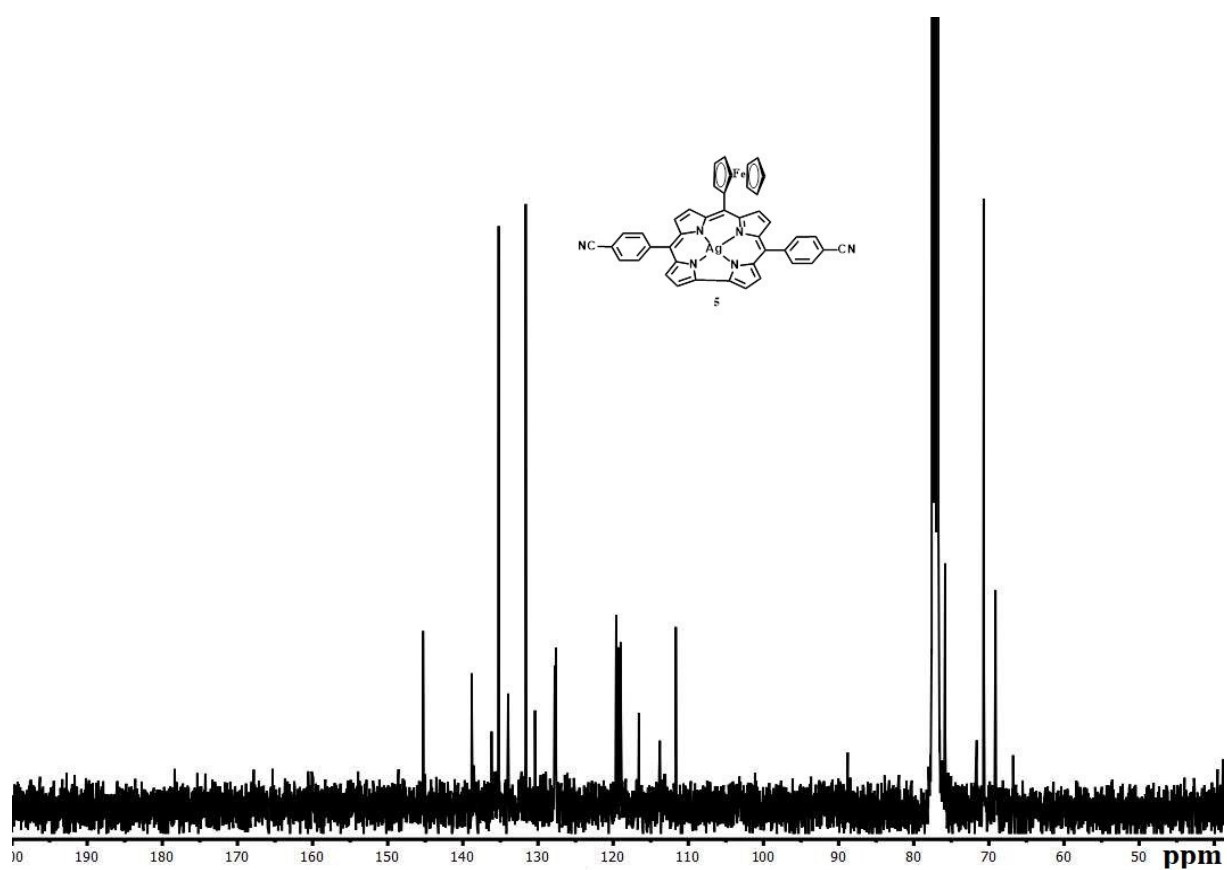


Fig. S4 ^{13}C NMR spectrum of 10-ferrocenyl-5,15-bis(4-cyanophenyl)corrolato-Ag(III), **5** in CDCl_3 .

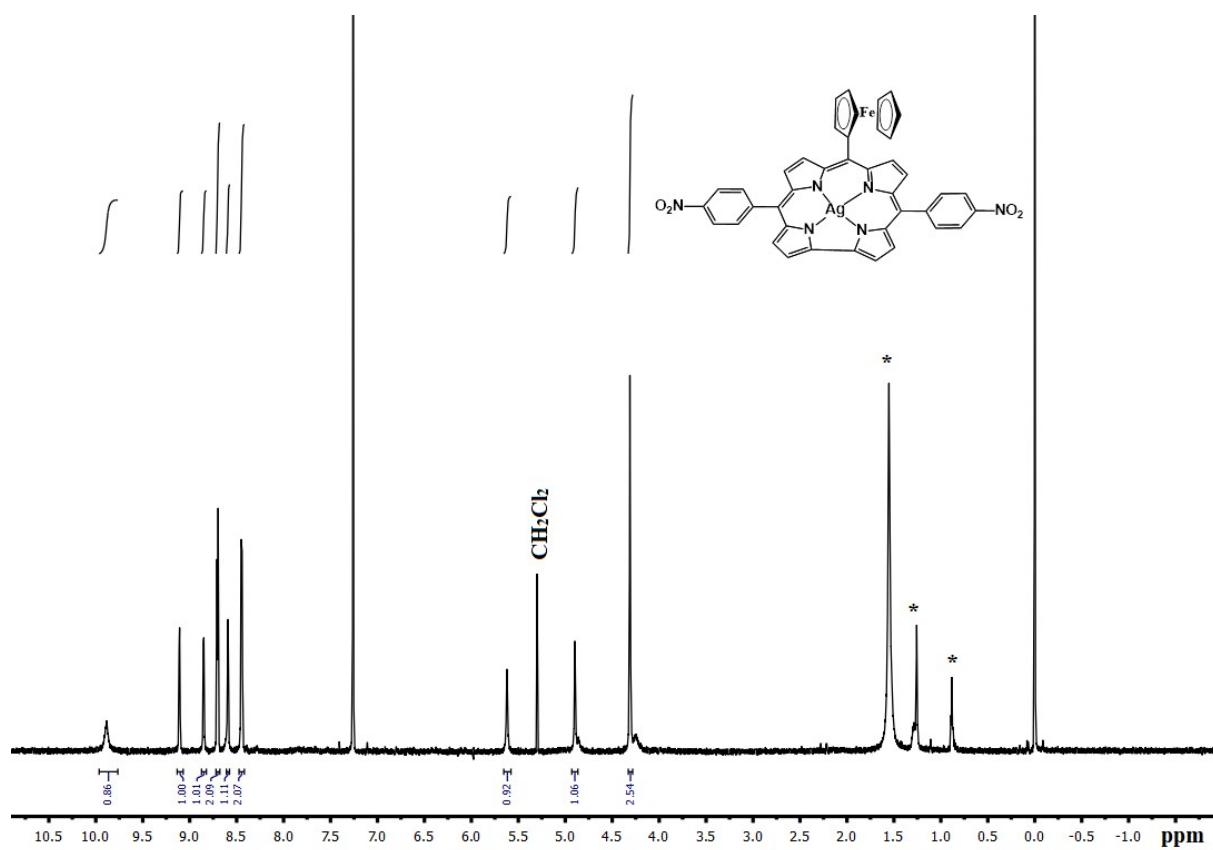


Fig. S5 ^1H NMR spectrum of 10-ferrocenyl-5,15-bis(4-nitrophenyl)corrolato-Ag(III), **6** in CDCl_3 .

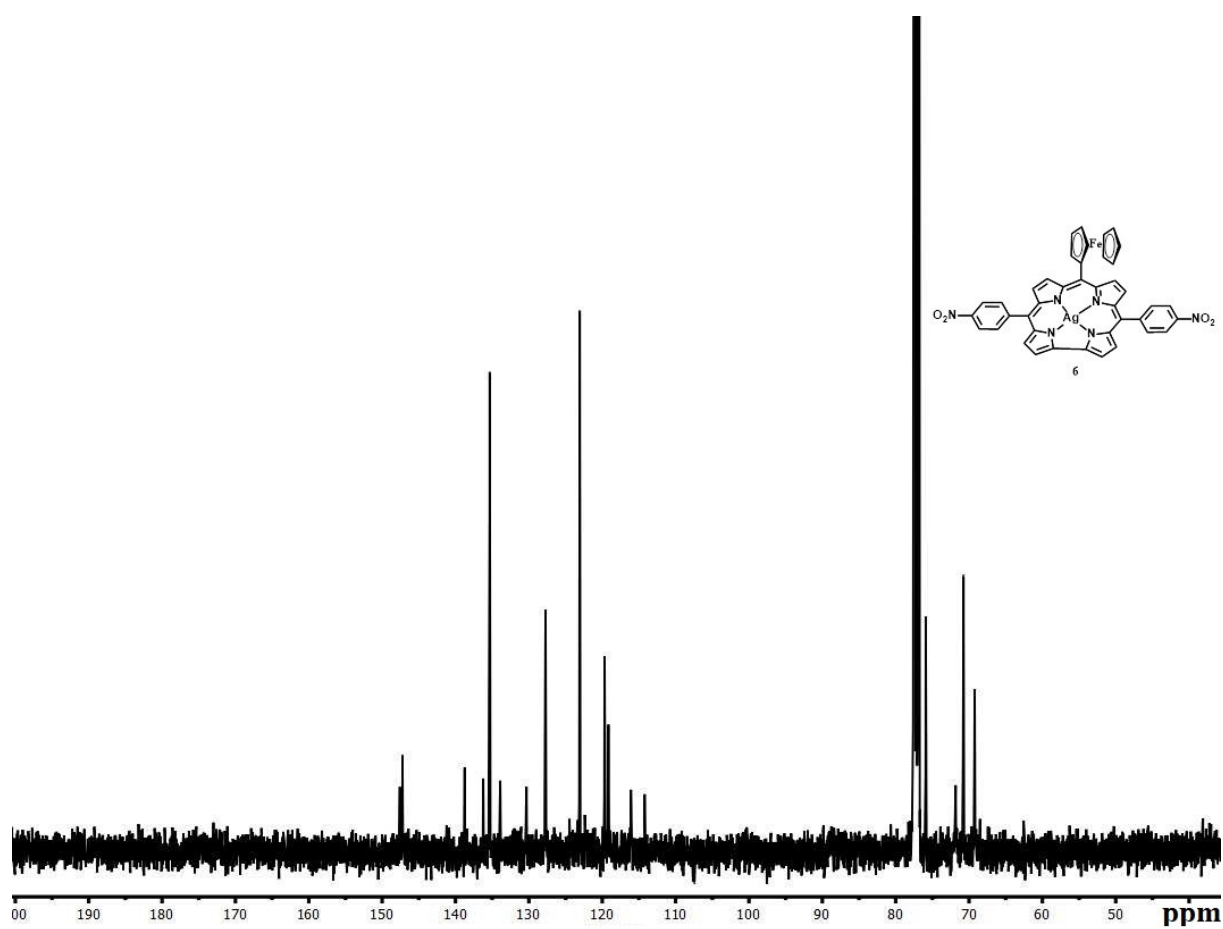


Fig. S6 ^{13}C NMR spectrum of 10-ferrocenyl-5,15-bis(4-nitrophenyl)corrolato-Ag(III), **6** in CDCl_3 .

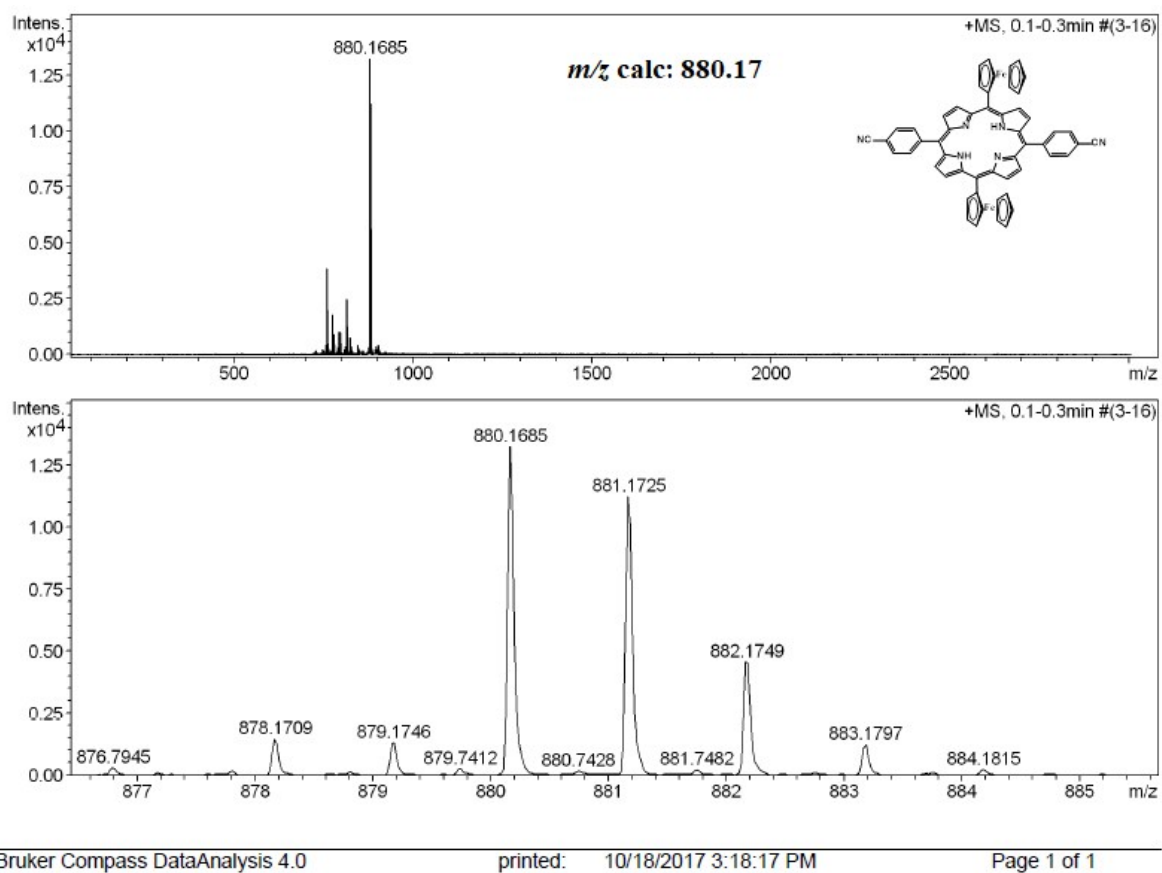


Fig. S7 ESI-MS spectrum of 5,15-diferrocenyl-10,20-bis(4-cyanophenyl)porphyrin, **1** in CH₃CN shows (a) the measured spectrum and (b) with isotopic distribution pattern.

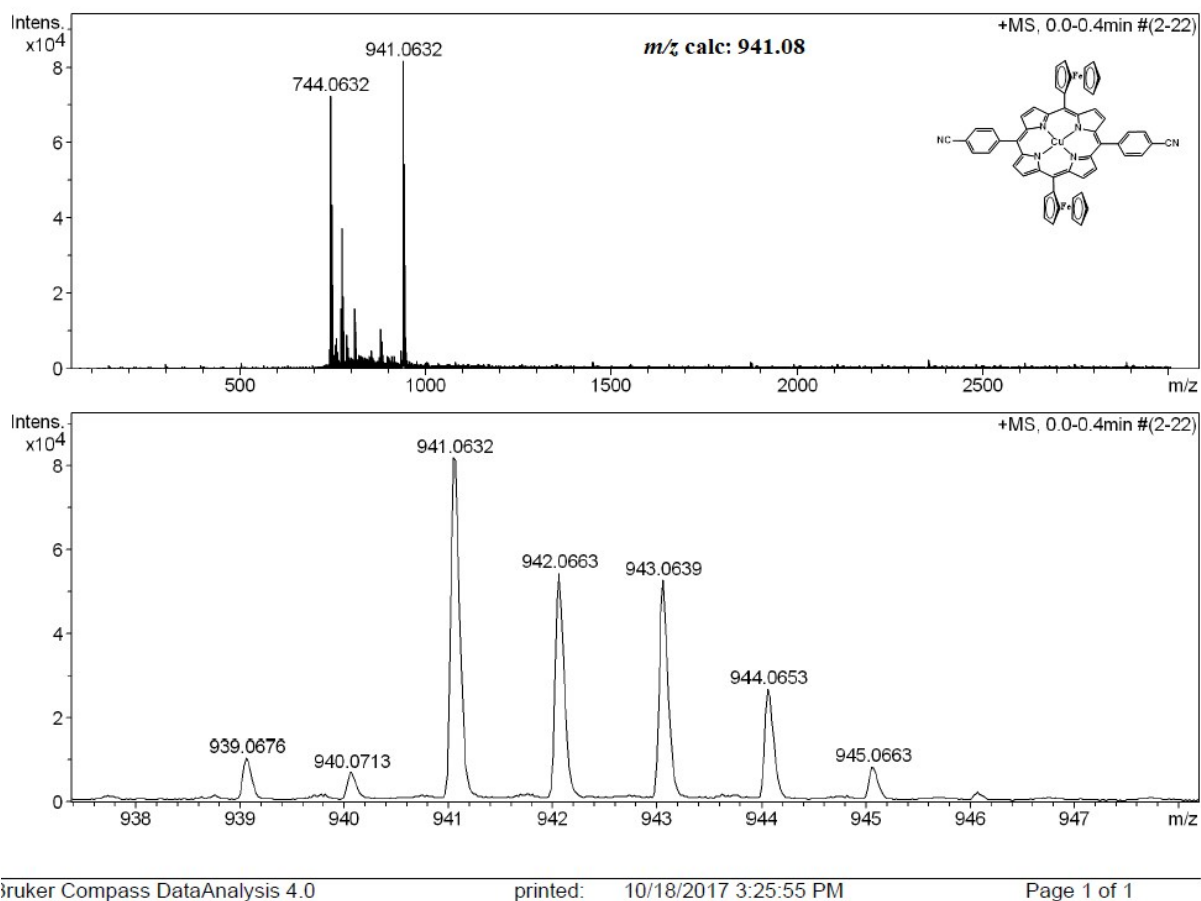


Fig. S8 ESI-MS spectrum of 5,15-diferrocenyl-10,20-bis(4-cyanophenyl)porphyrinato-Cu(II), **3** in CH_3CN shows (a) the measured spectrum and (b) with isotopic distribution pattern.

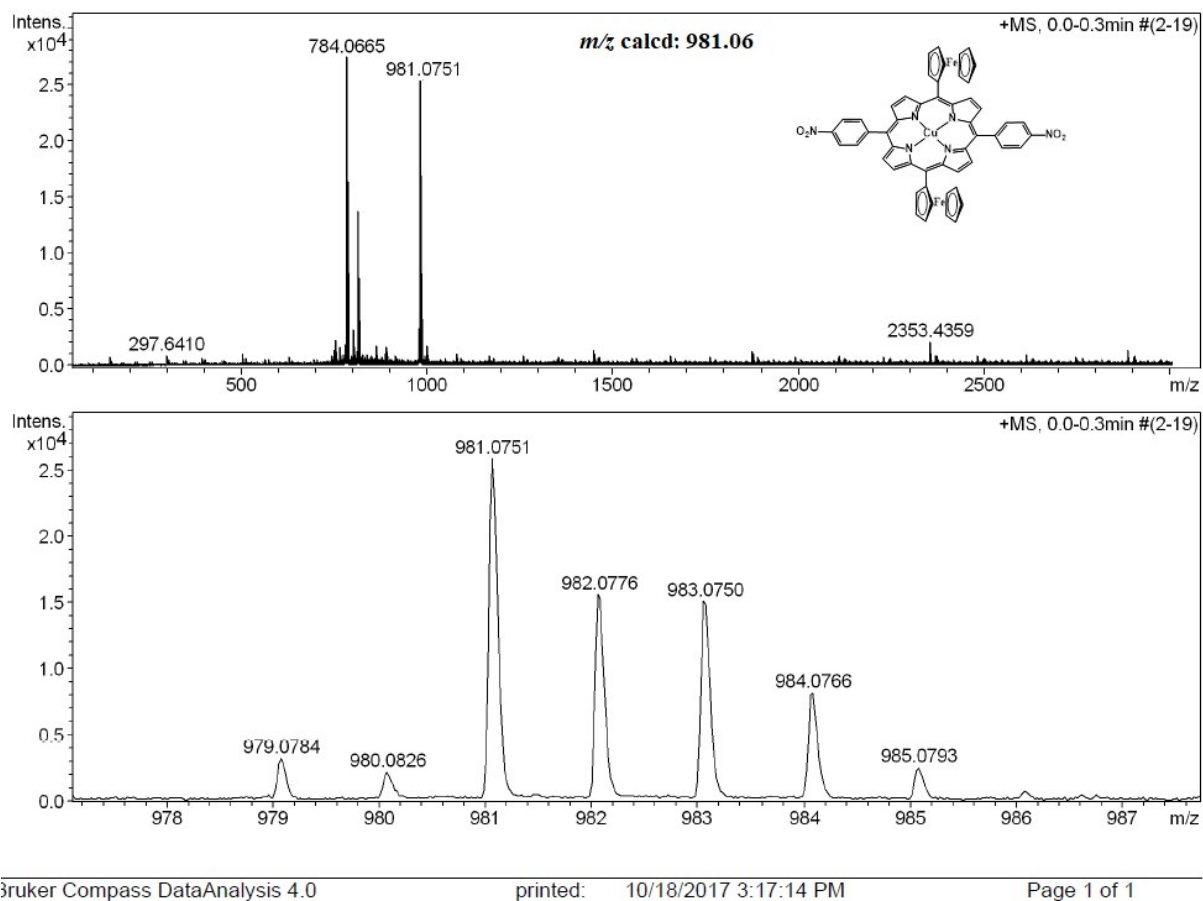


Fig. S9 ESI-MS spectrum of 5,15-diferrocenyl-10,20-bis(4-nitrophenyl)porphyrinato-Cu(II), **4** in CH₃CN shows (a) the measured spectrum and (b) with isotopic distribution pattern.

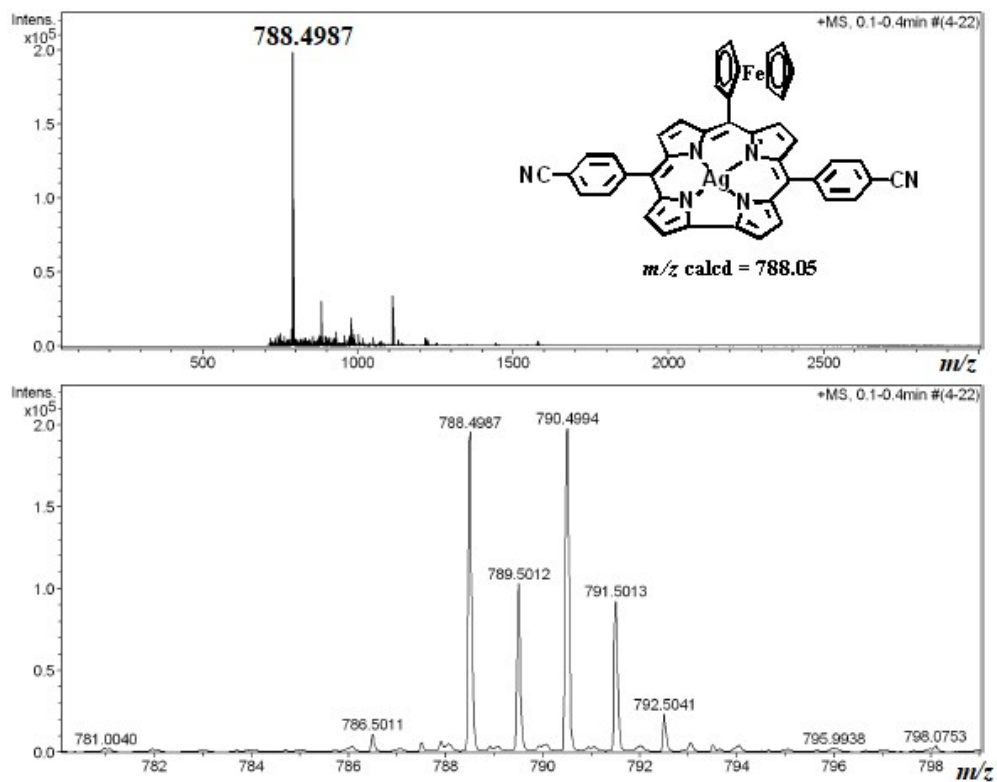


Fig. S10 ESI-MS spectrum of 10-ferrocenyl-5,15-bis(4-cyanophenyl)corrolato-Ag(III), **5** in CH₃CN shows (a) the measured spectrum and (b) with isotopic distribution pattern.

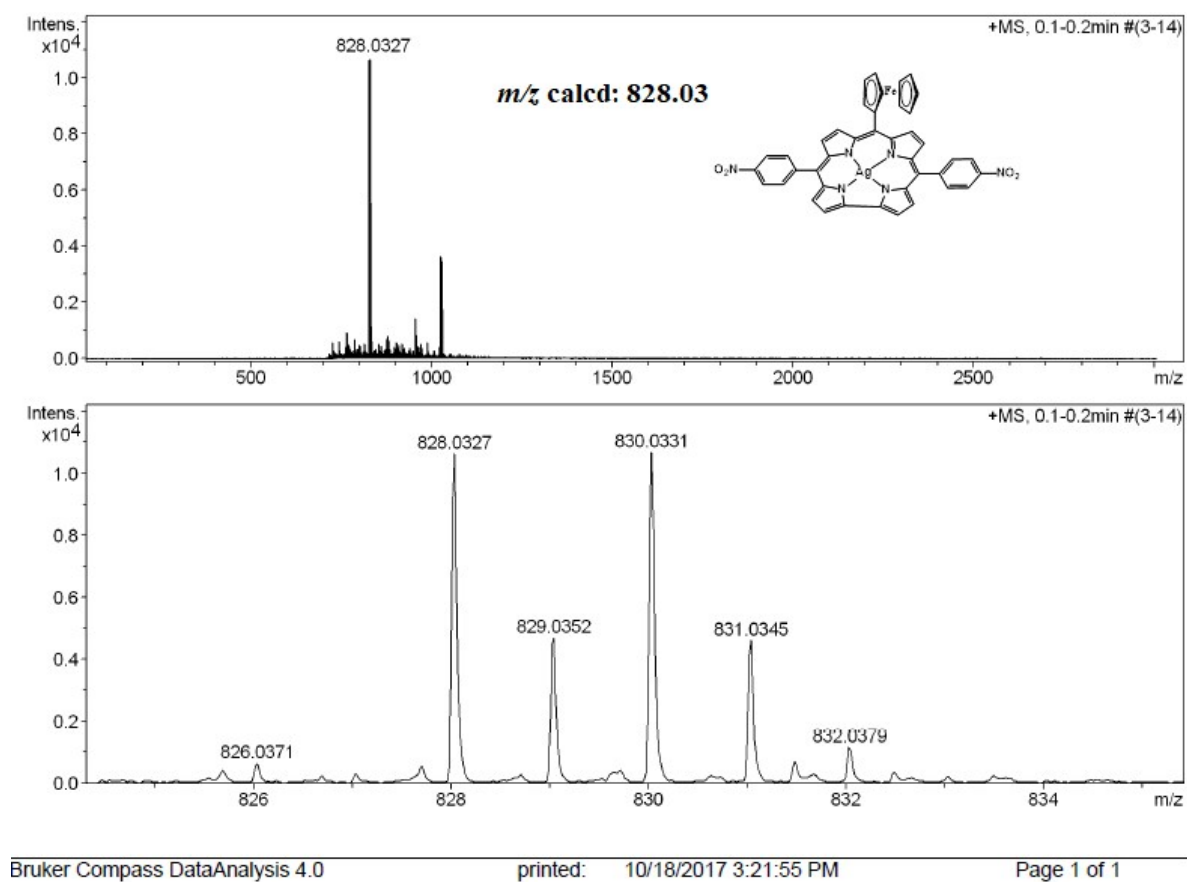


Fig. S11 ESI-MS spectrum of 10-ferrocenyl-5,15-bis(4-nitrophenyl)corrolato-Ag(III), **6** in CH₃CN shows (a) the measured spectrum and (b) with isotopic distribution pattern.

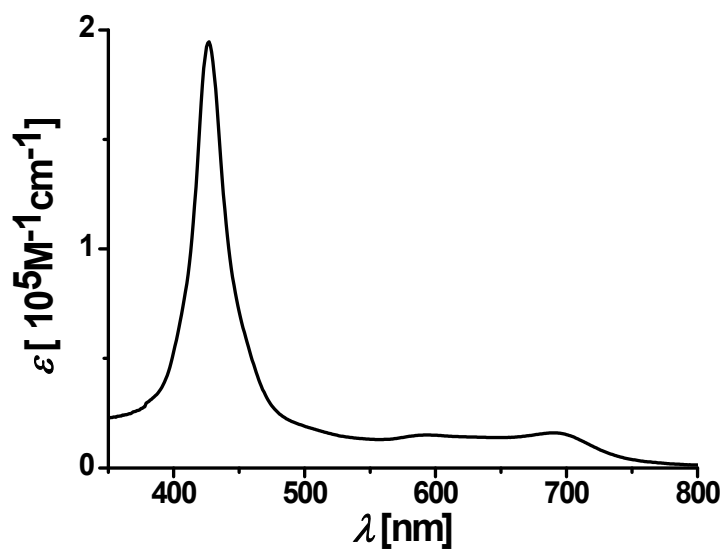


Fig. S12 Electronic absorption spectrum of **1** in dichloromethane.

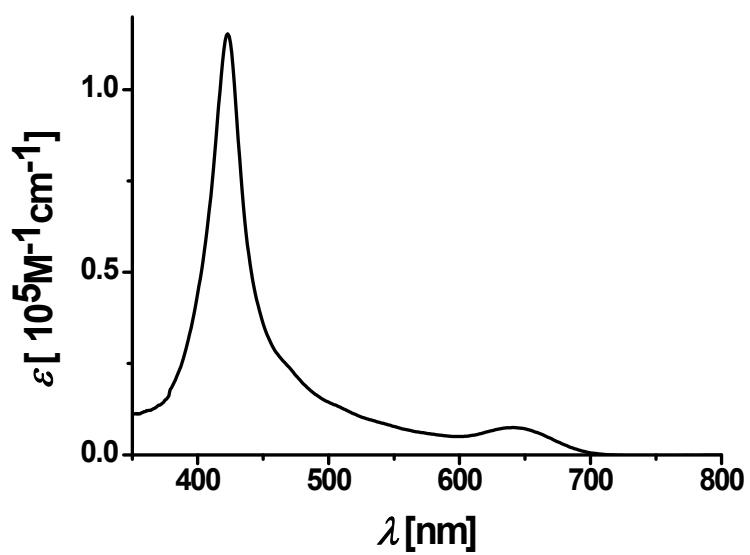


Fig. S13 Electronic absorption spectrum of **3** in dichloromethane.

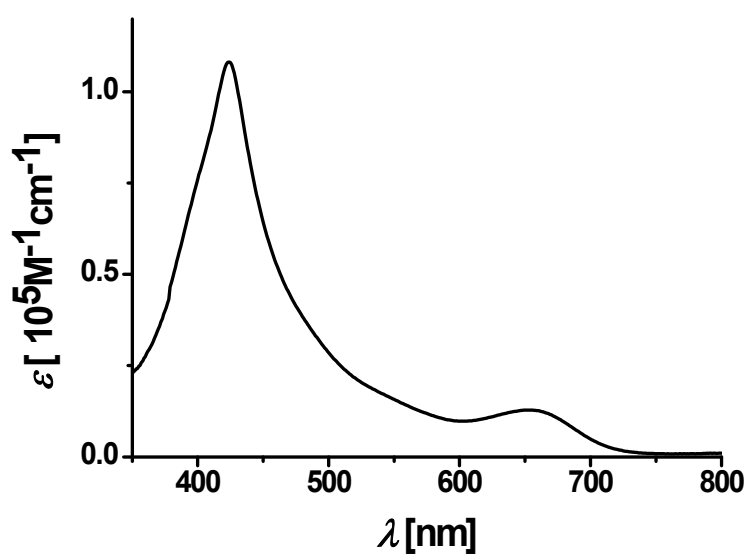


Fig. S14 Electronic absorption spectrum of **4** in dichloromethane.

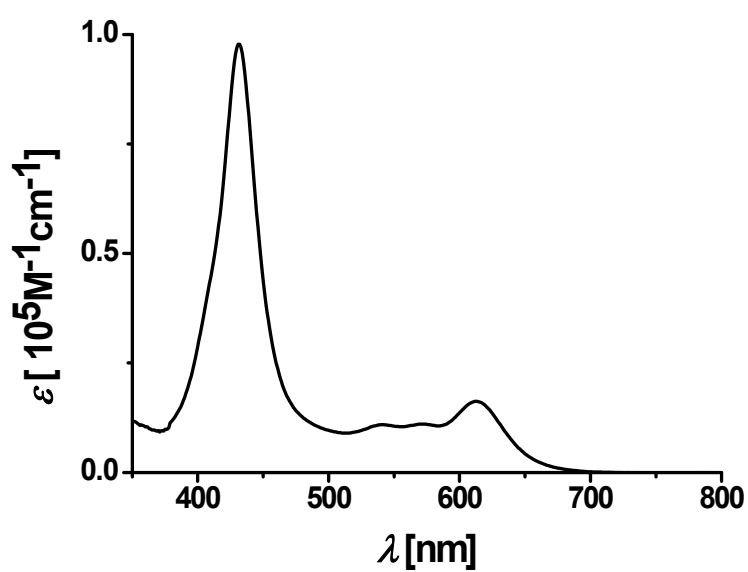


Fig. S15 Electronic absorption spectrum of **5** in dichloromethane.

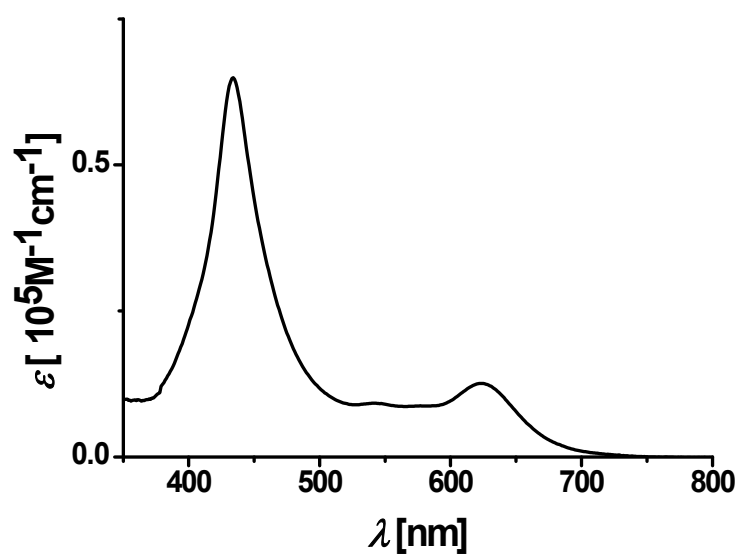


Fig. S16 Electronic absorption spectrum of **6** in dichloromethane.

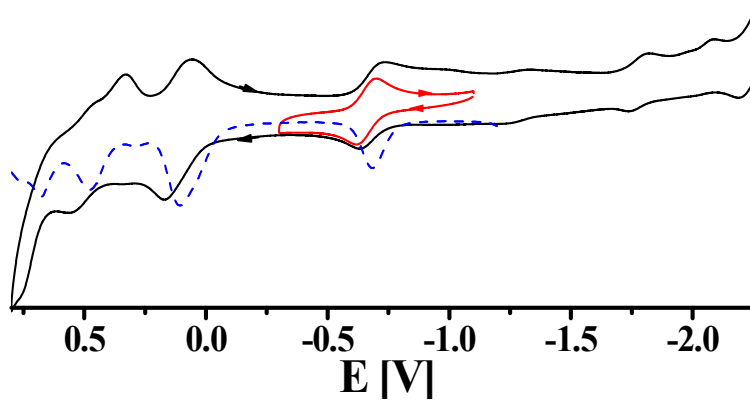


Fig. S17 Cyclic voltammograms (—) and differential pulse voltammograms (-·-·-·-) of **3** in CH₂Cl₂. The potentials are vs. ferrocene/ferricinium.

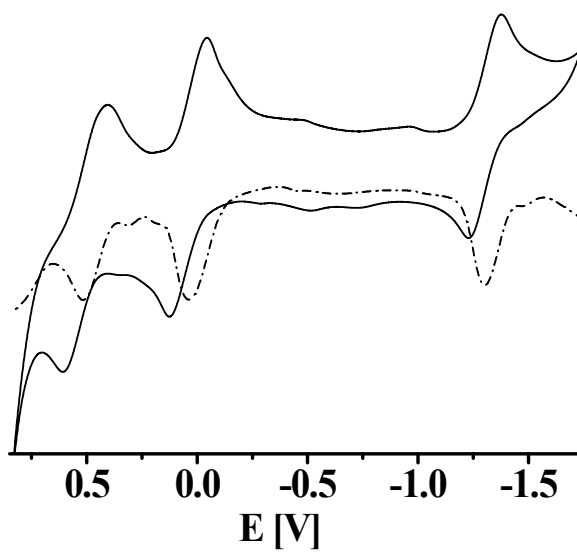


Fig. S18 Cyclic voltammograms (—) and differential pulse voltammograms (-·-·-·-) of **5** in CH₂Cl₂. The potentials are vs. ferrocene/ferricinium.

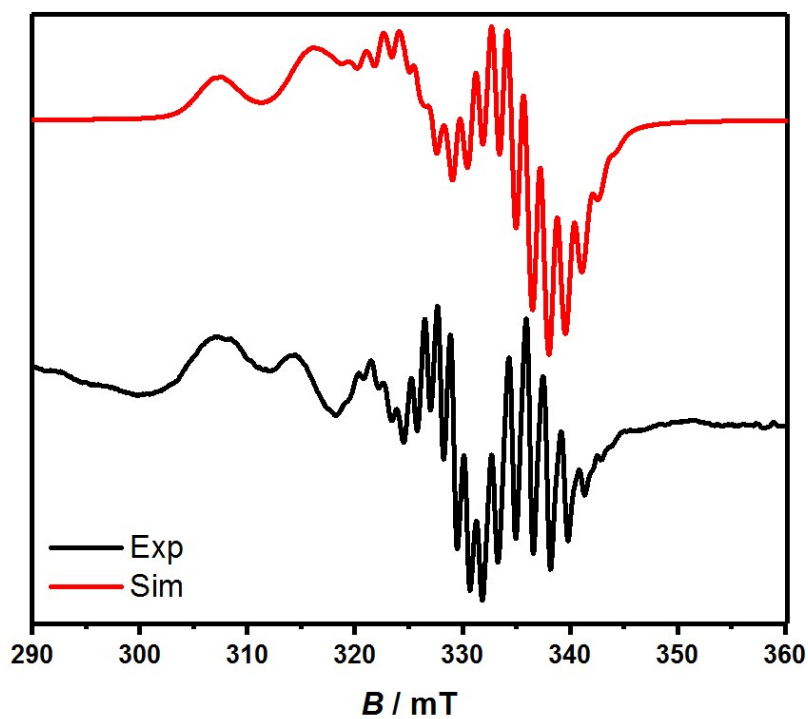


Fig. S19 Experimental and simulated EPR spectrum of **3** measured in DCM at room temperature.

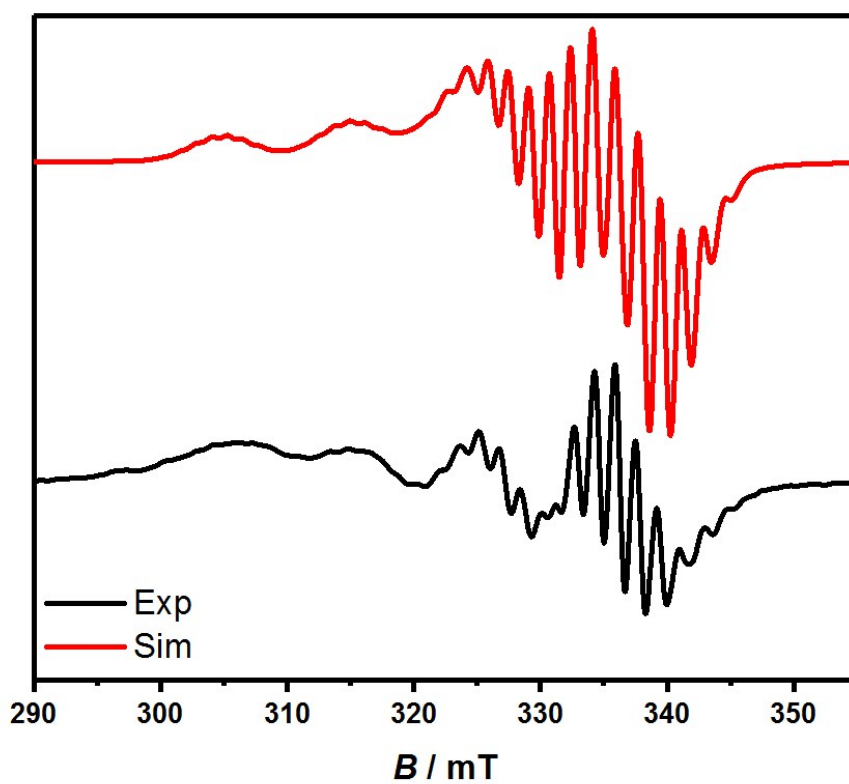


Fig. S20 Experimental and simulated EPR spectrum of **4** measured in DCM at room temperature.

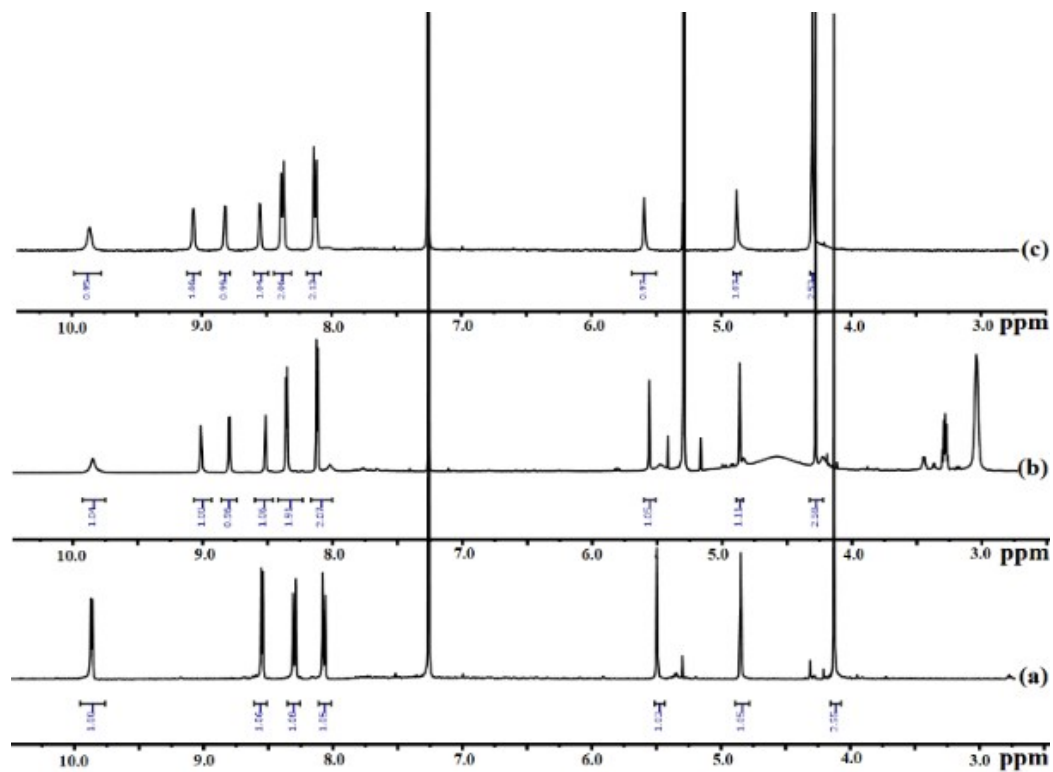


Fig. S21 ^1H NMR spectra of (a) pure **1** in CDCl_3 , (b) the sample prepared via treatment of **1** (equimolar amount) with $\text{Ag}(\text{CH}_3\text{COO})$ and trimethylamine in DCM, stirred at RT for 30 mins, followed by filtration of the silver residues and the evaporation of the residual solvent containing triethylamine and dissolution in CDCl_3 , and (c) pure **5** in CDCl_3 .

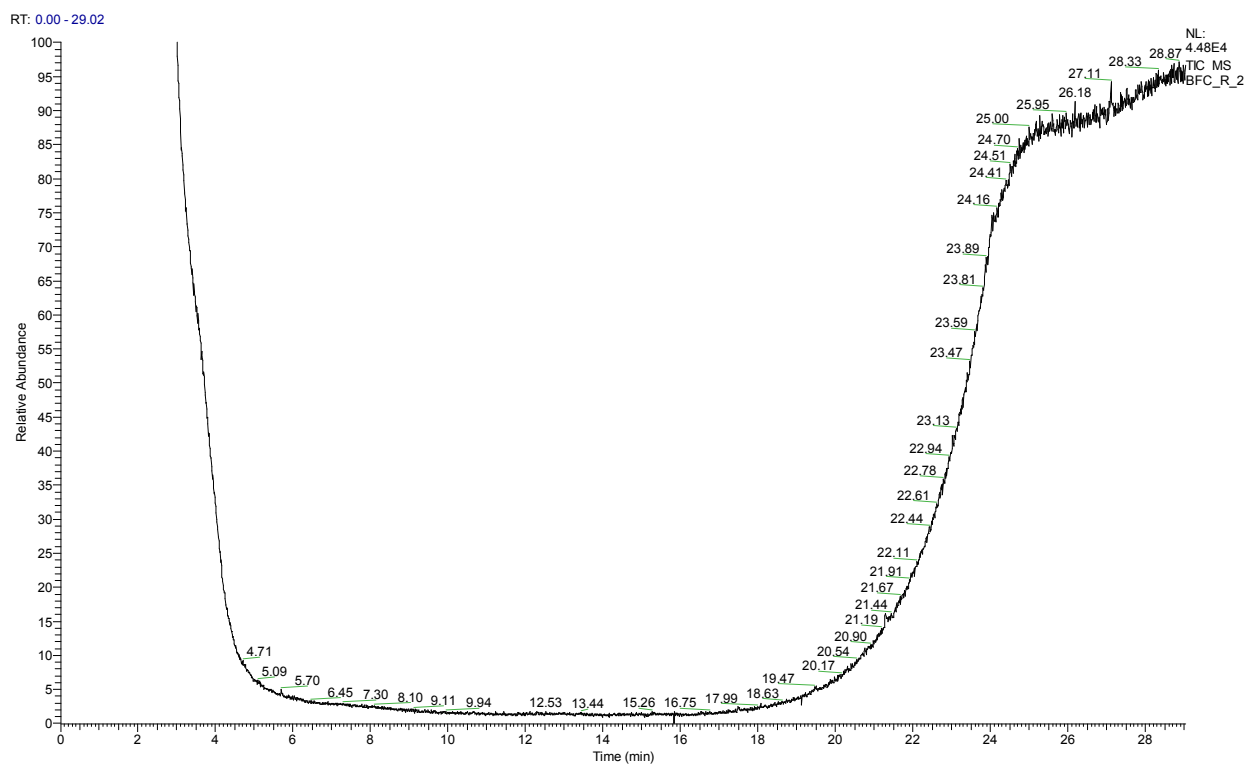


Fig. S22 5,15-diferrocenyl-10,20-bis(4-cyanophenyl)porphyrin, **1** was dissolved in dichloromethane. Then triethylamine was added to the reaction mixture and it was stirred continuously at room temperature. Aliquots of this reaction mixture were taken after 15 minutes and were monitored by GC-EIMS analysis.

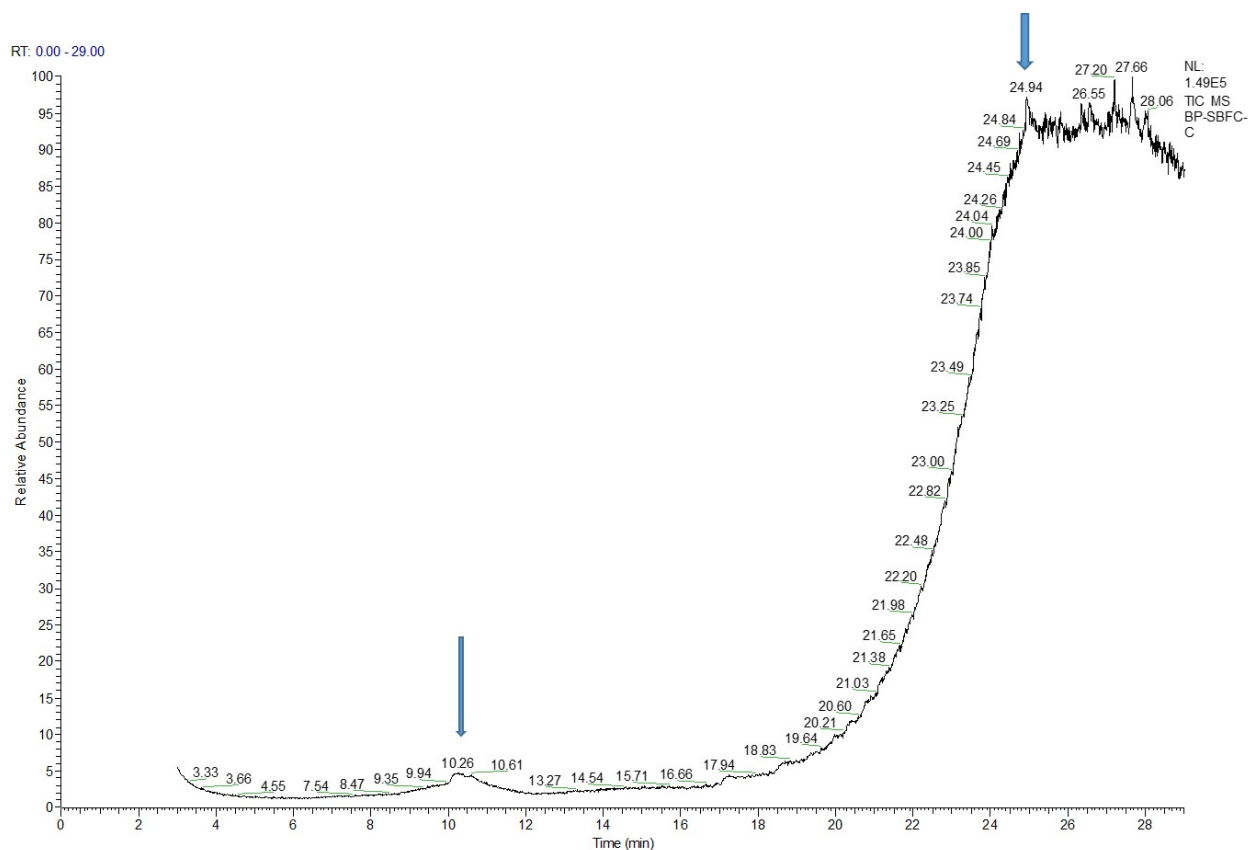


Fig. S23 5,15-diferrocenyl-10,20-bis(4-cyanophenyl)porphyrin, **1** was dissolved in dichloromethane and subsequently silver acetate was added to it. Then triethylamine was added to the reaction mixture and it was stirred continuously at room temperature. Aliquots of this reaction mixture were taken after 2 minutes and were monitored by GC-EIMS analysis.

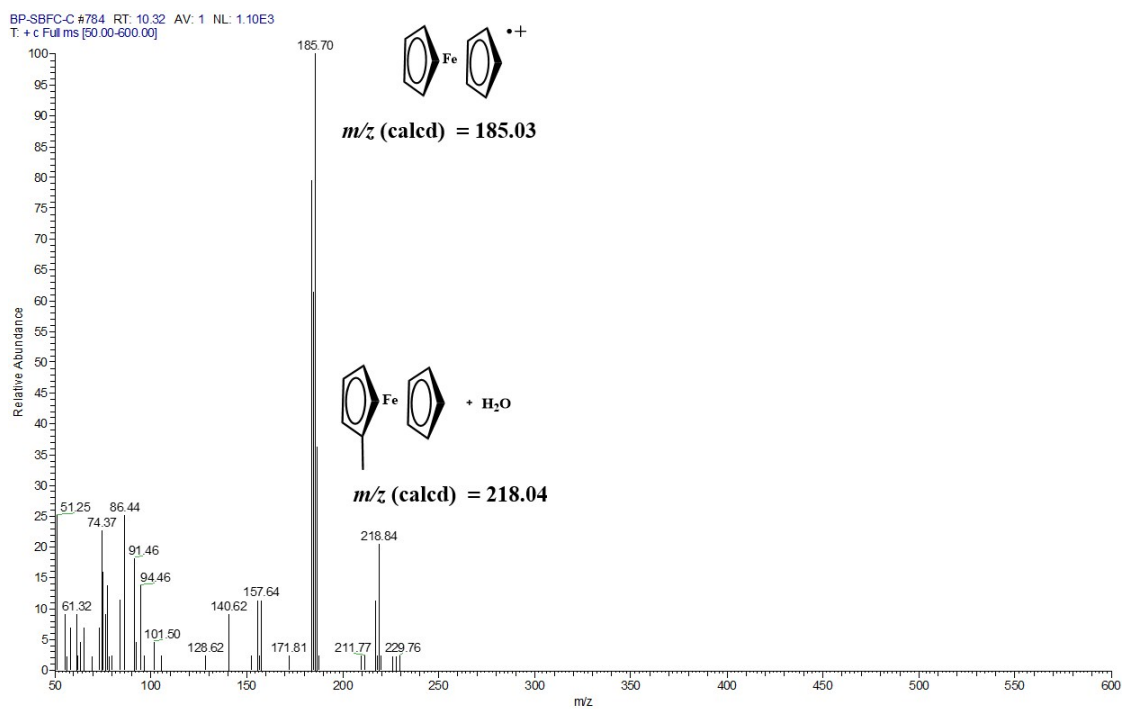


Fig. S24 Mass spectrum (GC-EIMS) of ferrocenyl derivatives detected by GC of the reaction mixture.

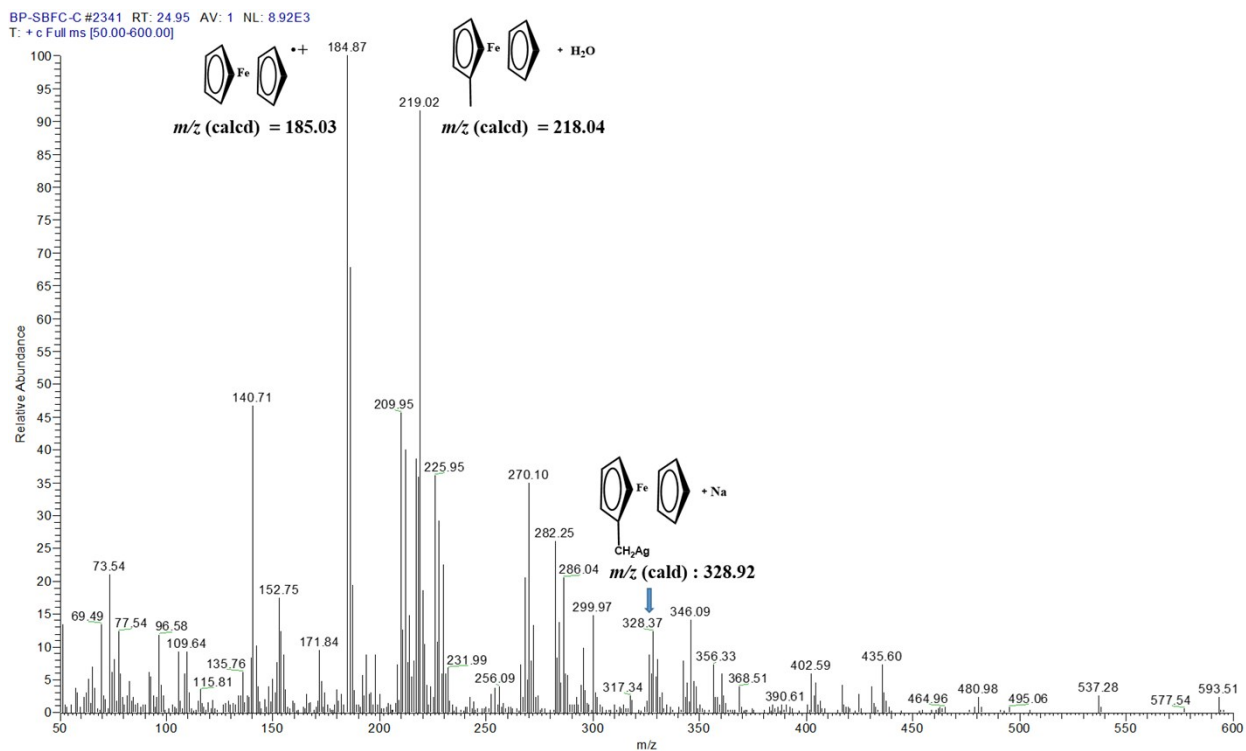


Fig. S25 Mass spectrum (GC-EIMS) of ferrocenyl derivatives detected by GC of the reaction mixture.

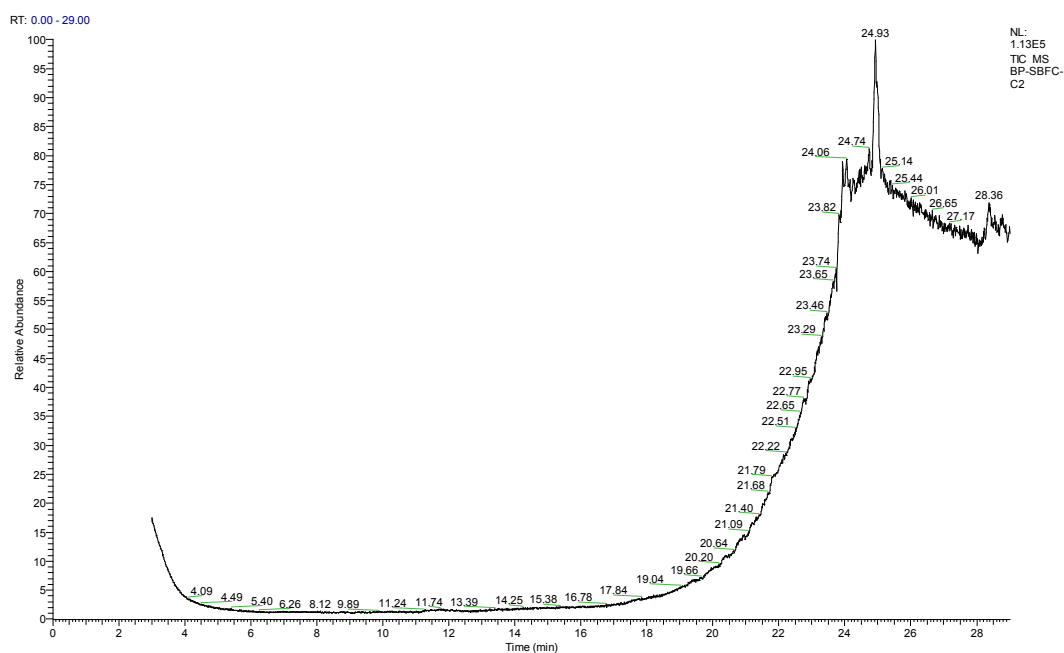


Fig. S26 5,15-diferrocenyl-10,20-bis(4-cyanophenyl)porphyrin, **1** was dissolved in dichloromethane and subsequently silver acetate was added to it. Then triethylamine was added to the reaction mixture and it was stirred continuously at room temperature. Aliquots of this reaction mixture were taken after 30 minutes and were monitored by GC-EIMS analysis.

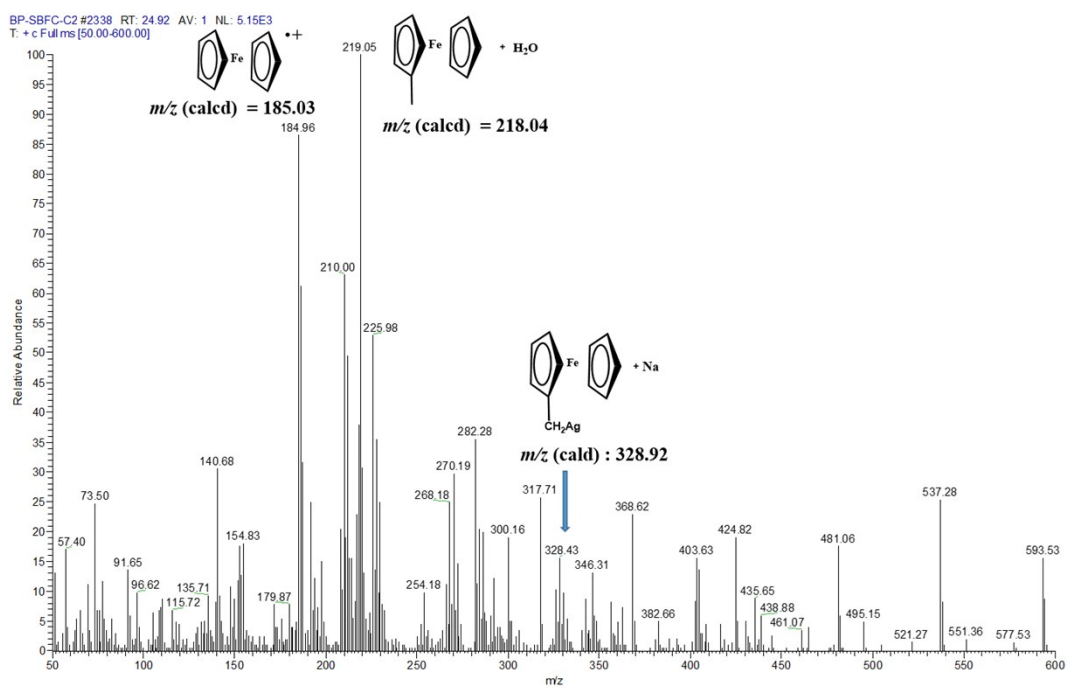


Fig. S27 Mass spectrum (GC-EIMS) of ferrocenyl derivatives detected by GC of the reaction mixture.

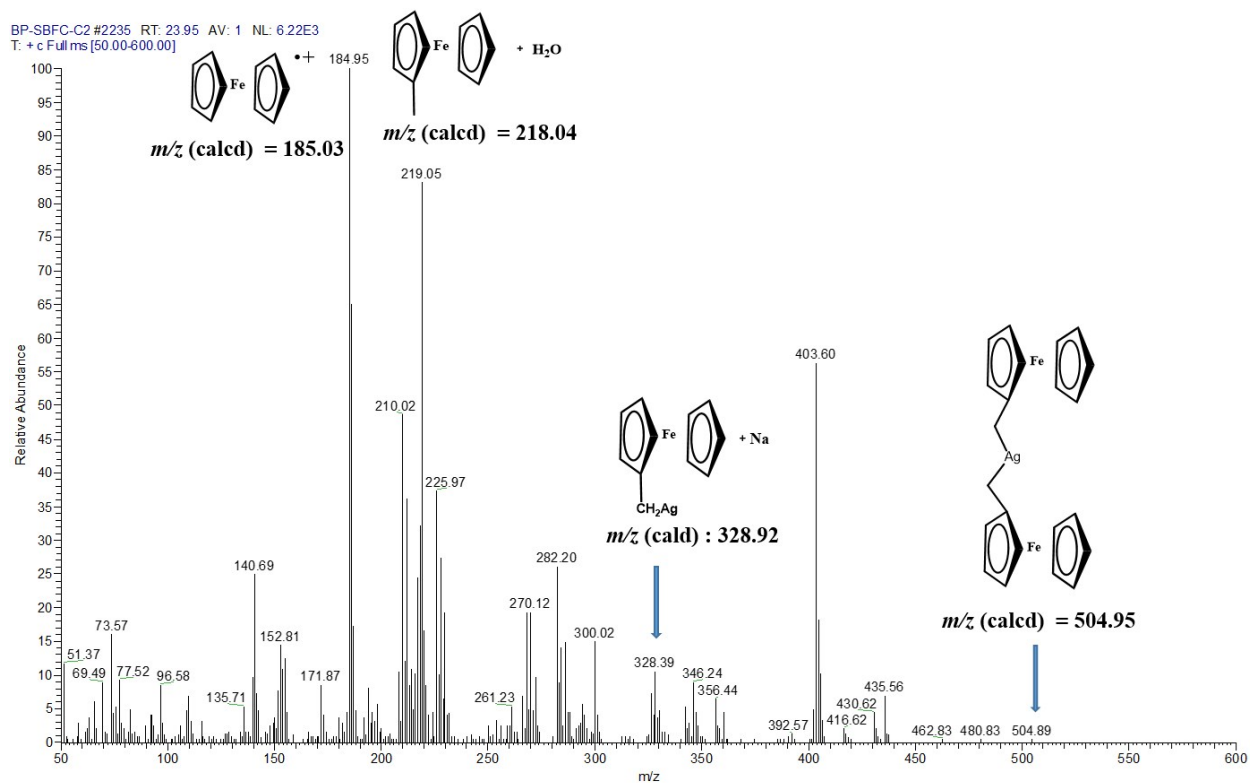


Fig. S28 Mass spectrum (GC-EIMS) of ferrocenyl derivatives detected by GC of the reaction mixture.

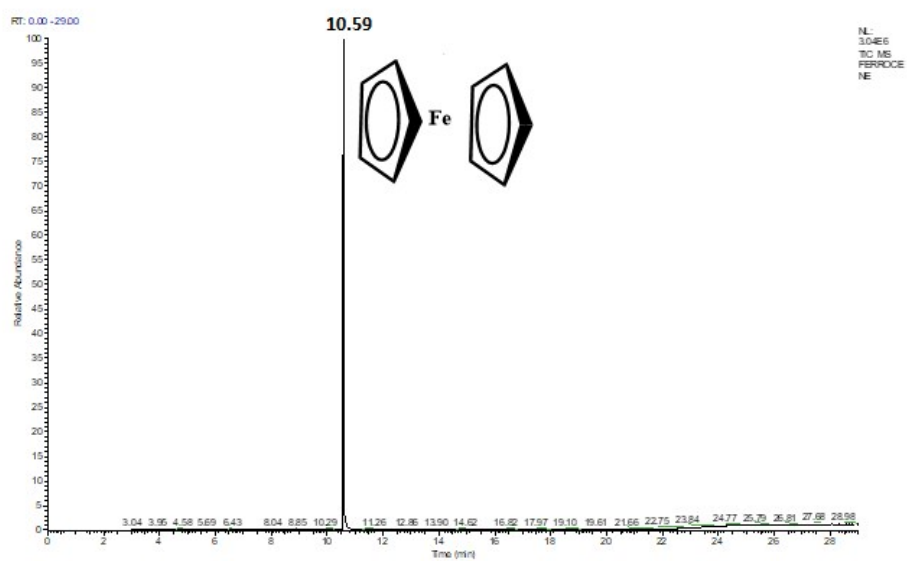


Fig. S29 Ferrocene was dissolved in dichloromethane and were monitored by GC-EIMS analysis.

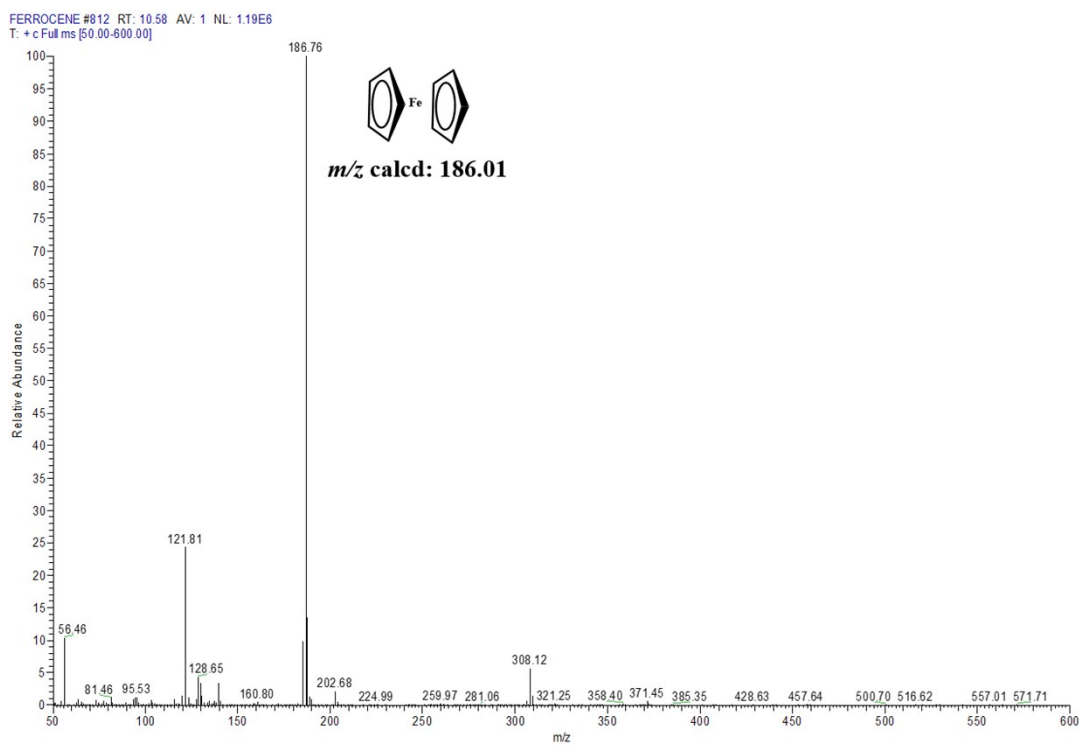


Fig. S30 Mass spectrum (GC-EIMS) of ferrocene detected by GC of the reaction mixture.

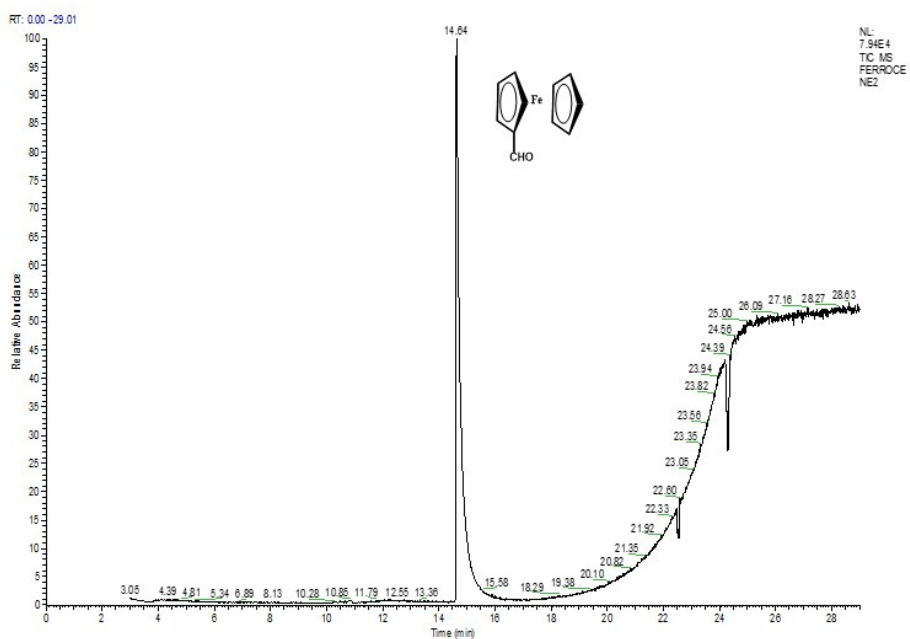


Fig. S31 Ferrocenecarboxaldehyde was dissolved in dichloromethane and were monitored by GC-EIMS analysis.

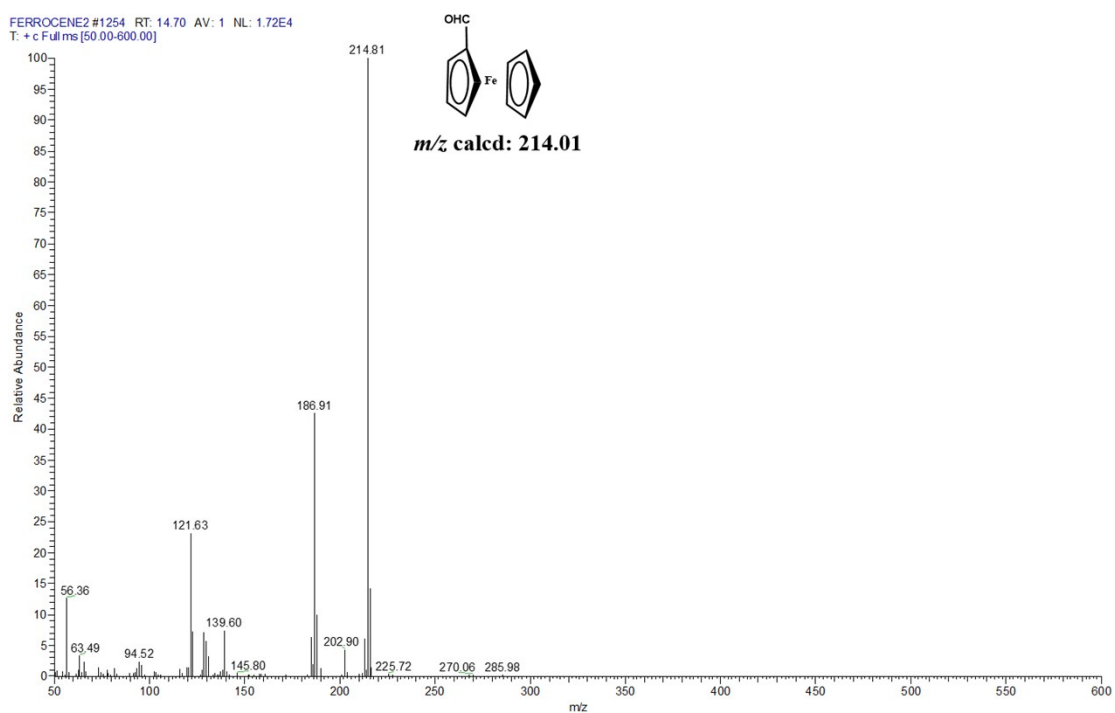


Fig. S32 Mass spectrum (GC-EIMS) of ferrocenecarboxaldehyde detected by GC of the reaction mixture.

Table S1 Crystallographic Data for **3** and **5**.

| compound codes | 3 | 5 |
|--|--|--|
| molecular formula | C ₅₄ H ₃₄ CuFe ₂ N ₆ | 3(C ₄₃ H ₂₅ AgFeN ₆) |
| Fw | 942.11 | 3 × 789.41 |
| Radiation | MoK α | Cu K α |
| crystal symmetry | Monoclinic | Triclinic |
| space group | <i>P</i> 2 ₁ / <i>c</i> | P -1 |
| <i>a</i> (Å) | 18.6124(8) | 18.4767(6) |
| <i>b</i> (Å) | 8.9540(4) | 18.7775(7) |
| <i>c</i> (Å) | 15.5768(7) | 19.6170(5) |
| α (deg) | 90 | 99.222(2) |
| β (deg) | 113.979(2) | 104.379(2) |
| γ (deg) | 90 | 117.221(4) |
| <i>V</i> (Å ³) | 2371.91(18) | 5558.5(4) |
| <i>Z</i> | 2 | 2 |
| μ (mm ⁻¹) | 1.089 | 7.677 |
| <i>T</i> (K) | 296 | 298 |
| <i>D</i> _{calcd} (g cm ⁻³) | 1.319 | 1.415 |
| 2 θ range (deg) | 2.395 to 26.057 | 2.452 to 66.999 |
| <i>e</i> data (<i>R</i> _{int}) | 4676 (0.087) | 19796 (0.058) |
| R1 (<i>I</i> > 2 σ (<i>I</i>)) | 0.0438(2799) | 0.0533(16557) |
| WR2 (all data) | 0.0996(4676) | 0.1585(19796) |
| GOF | 0.957 | 1.169 |
| $\Delta\rho_{\max}$, $\Delta\rho_{\min}$ (e Å ⁻³) | 0.34, -0.32 | 2.510, -1.320 |

Table S2 UV–Vis. and electrochemical data

| Compound | UV–vis. Data ^a λ_{max} / nm (ϵ / M ⁻¹ cm ⁻¹) | Electrochemical data ^a | |
|----------|--|---|---|
| | | Oxidation E^0 , V (ΔE_p , mV) | Reduction E^0 , V (ΔE_p , mV) |
| 1 | 427 (195000), 593 (15000), 690 (16000). | 0.04 (80), 0.16 (70). | - |
| 2 | 428 (93000), 606 (18500), 695 (19000). | | |
| 3 | 423 (115000), 642 (7500). | 0.12 (100), 0.49 (90). | -0.64 (80). |
| 4 | 423 (108000), 653 (13000). | | |
| 5 | 431 (98000), 541 (11000), 571 (11000), 612 (16000). | 0.05 (80), 0.51 (100). | -1.30 (100). |
| 6 | 434 (65000), 542 (9200), 577 (8800), 624 (12700). | | |

^a In dichloromethane.

The potentials are vs. ferrocene/ferricinium.

Table S3. Overview of g values and hyperfine coupling constants, obtained from simulation.

| | g_1 | g_2 | $A_1(^{63,65}\text{Cu})$ | $A_2(^{63,65}\text{Cu})$ | $A_1(^{14}\text{N})$ | $A_2(^{14}\text{N})$ |
|----------|-------|-------|--------------------------|--------------------------|----------------------|----------------------|
| 3 | 2.040 | 2.110 | 120 | 250 | 45 | 25 |
| 4 | 2.029 | 2.113 | 90 | 290 | 47 | 37 |